

Characterization of radiation induced defects in silicon devices

Michael Moll, CERN, Geneva, Switzerland

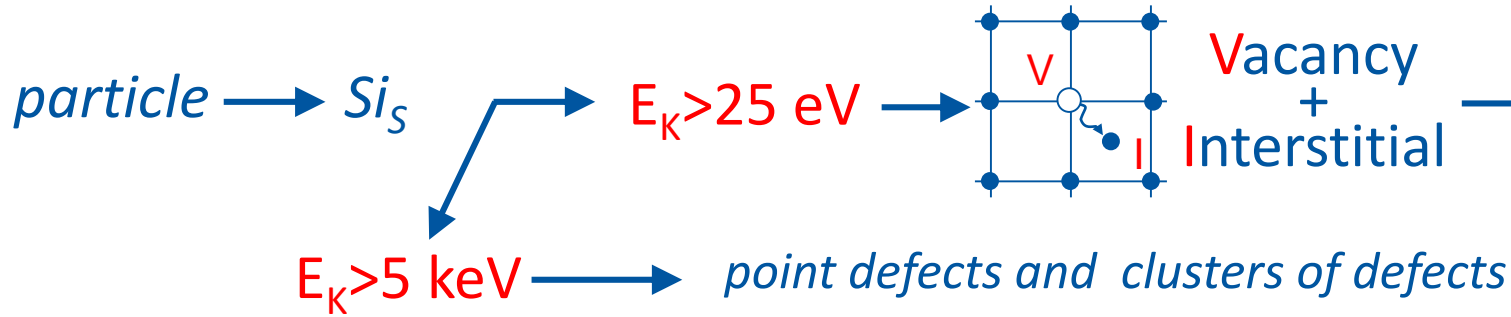
Outline:

- Introduction to radiation induced defects
- Characterization methods with examples
 - TSC, DLTS, PL, FTIR, EPR
- Microscopic Defects vs. Macroscopic Effects
 - Some results of the RD50 collaboration
- Summary

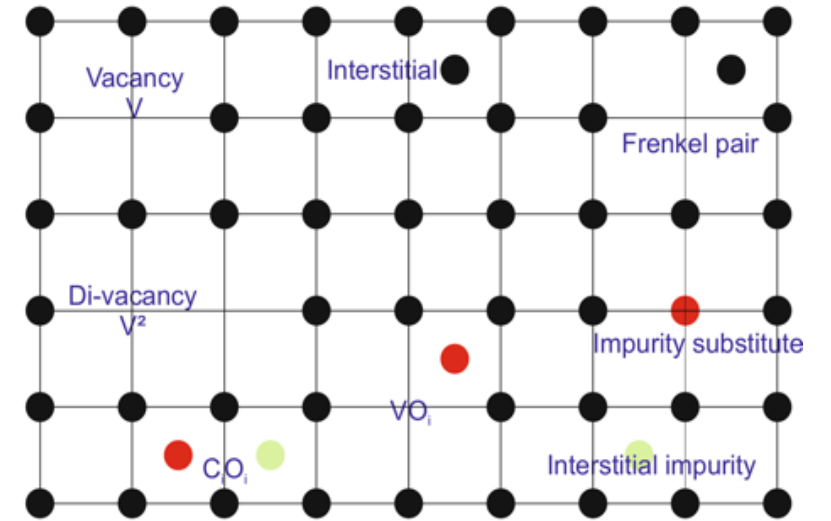


Radiation induced defects

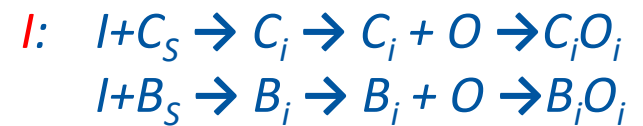
Displacement Damage



..... a wide range of point defects

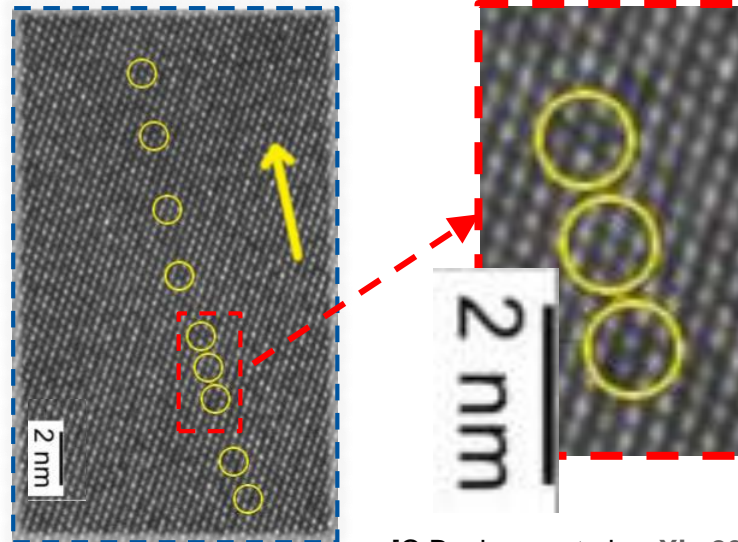


• example of point defect reactions:

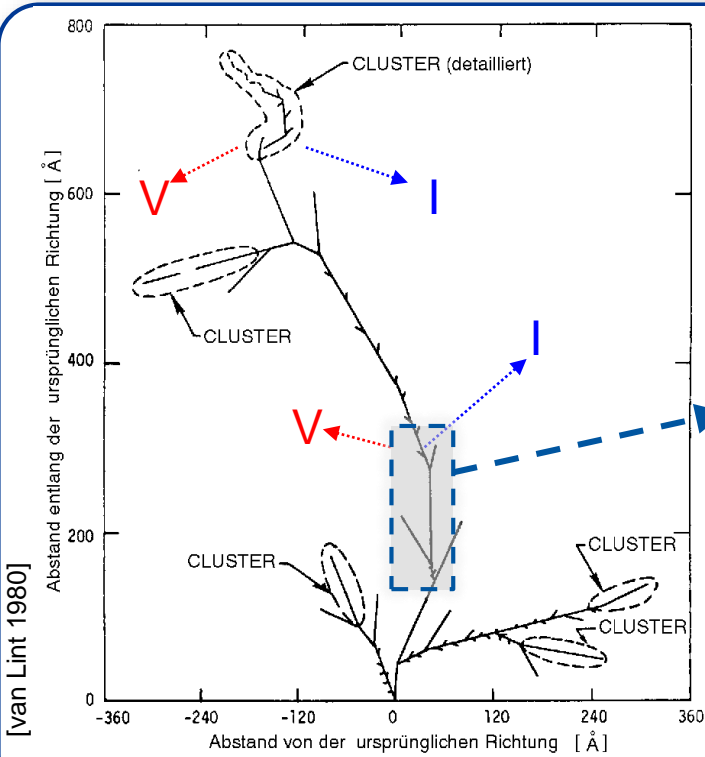


... many more reactions!

Can we see the defects?
 HRTEM on Si: n-irradiated $10^{19} n_{eq}/cm^2$
 High Resolution Transmission Electron Microscopy



[C.Besleaga et al. arXiv 2021]



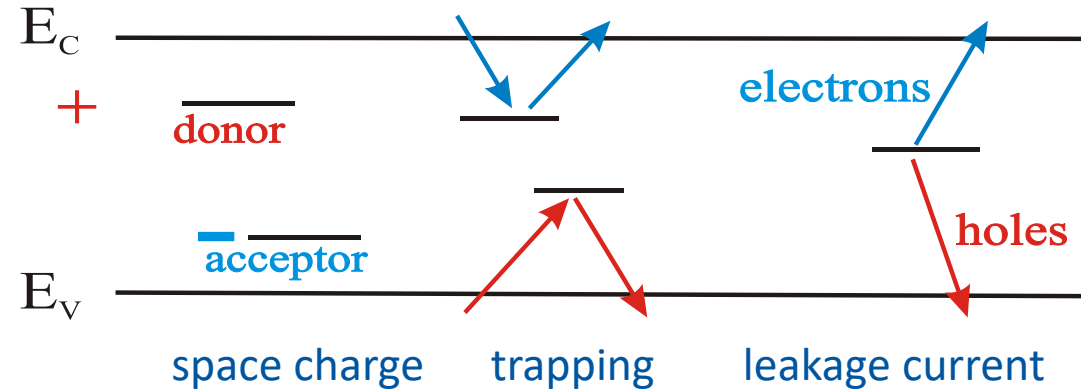
[van Lint 1980]

Defect Characterization



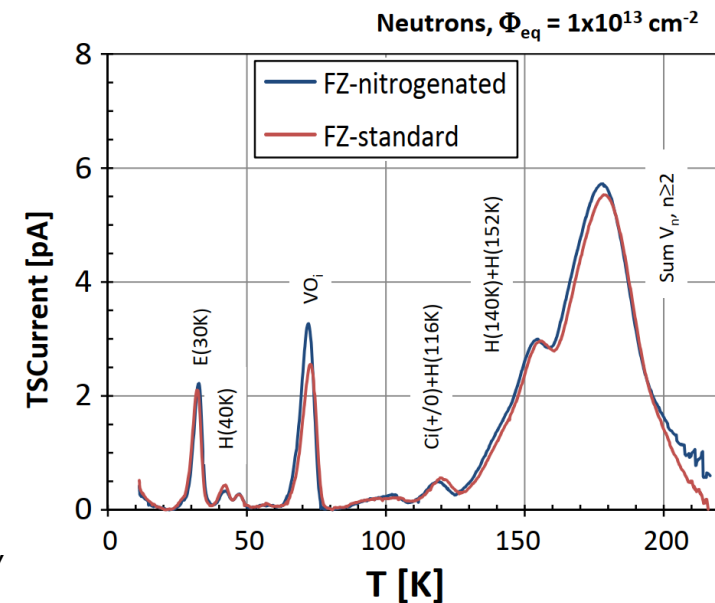
- Aim of defect studies:

- **Identify defects** responsible for Change of N_{eff} , Change of E-Field, Trapping, Leakage Current
- Understand if knowledge can be used to mitigate radiation damage (e.g. **defect engineering**)
- Deliver input for device simulations to **predict detector performance** under various conditions



- Defect Characterization performed with various tools:

- **DLTS** (Deep Level Transient Spectroscopy)
- **TSC** (Thermally Stimulated Currents)
- **PITS** (Photo Induced Transient Spectroscopy)
- **FTIR** (Fourier Transform Infrared Spectroscopy)
- **EPR** (Electron Paramagnetic Resonance)
- **TCT** (Transient Current Technique)
- **CV/IV** (Capacitance/Current-Voltage Measurement)
- **MW-PC** (Microwave Probed Photo Conductivity)
- **PC, PL, I-DLTS, TEM,...** and simulations
- RD50: several hundred samples irradiated with protons, neutrons, electrons, $^{60}\text{Co}-\gamma$



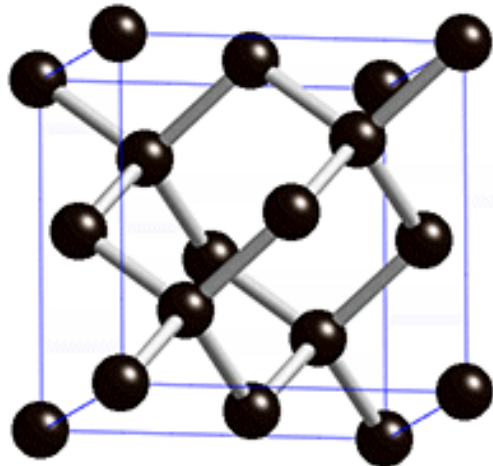
[E.Fretwurst et al. – RD50 Nov.2018]

Silicon Point Defects: The V-O defect (A center)



• Silicon crystal

- diamond lattice structure
- FCC: Face Centered Cubic



• V-O defect (A centre)

The dominant centres for vacancy capture in high purity silicon is the isolated oxygen interstitial O_i . Trapping of the vacancy results in the V-O centre, the so called A-centre.

Structure:

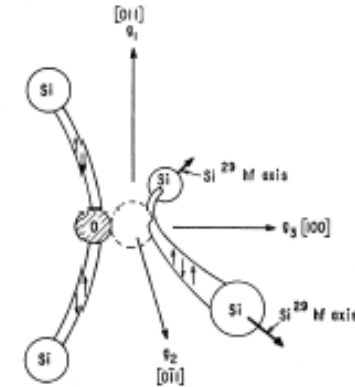
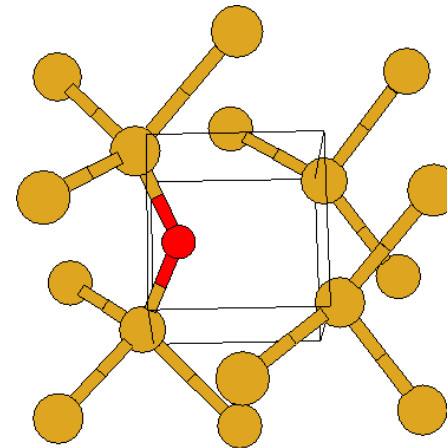
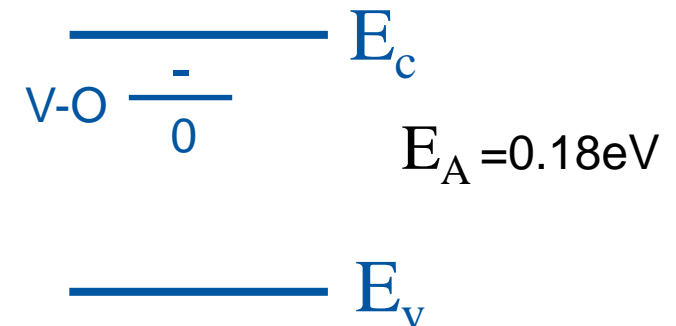


FIG. 5. Model of the A center as a substitutional oxygen atom. The oxygen atom bonds between two of the four neighboring silicon atoms, and the remaining two silicon atoms pull together to form a covalent bond. Spin resonance arises from an additional electron which is trapped in the Si-Si molecular bond as shown. The g tensor and hyperfine axes are indicated.

Electrical activity:

The A center has an acceptor level in the upper half of the band gap



Watkins, Corbett: Phys.Rev., 121, 4, (1961), 1001

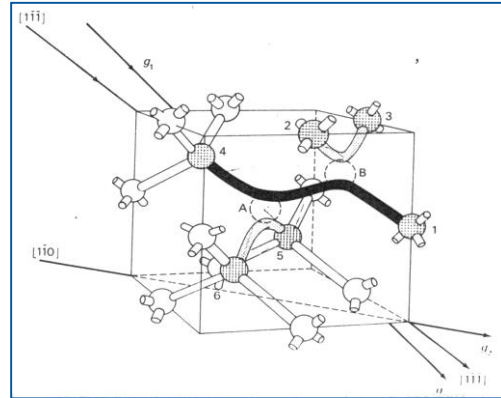
Silicon Point Defects: The Divacancy V_2



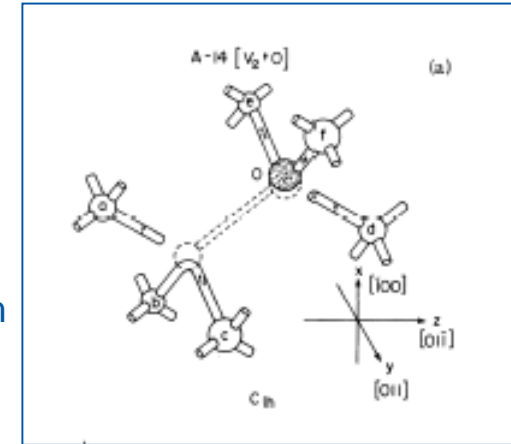
Point defects can involve more than one vacancy

- V_2 , V_3 , V_2O , V_2O_2 are well characterized defects

Divacancy V_2
two missing silicon atoms

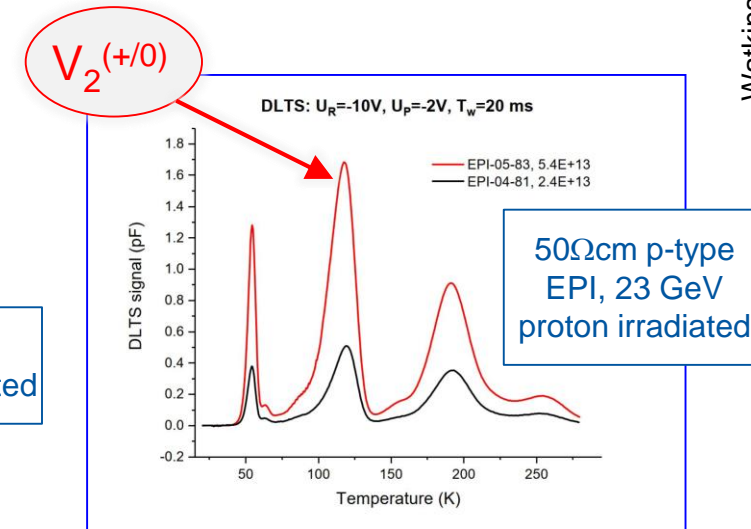
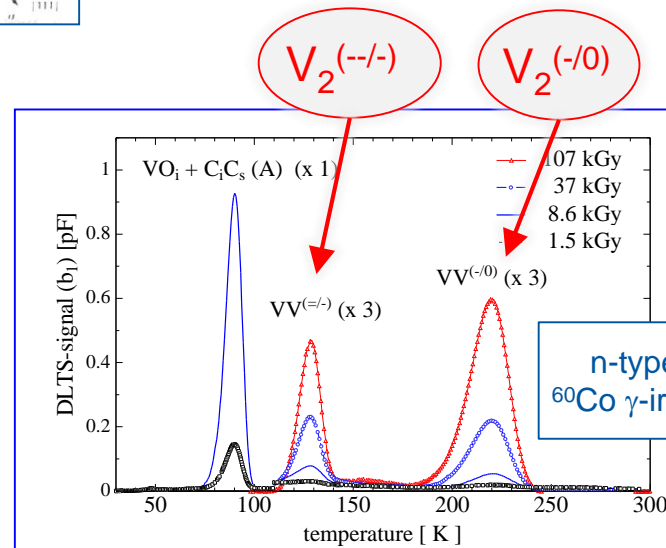
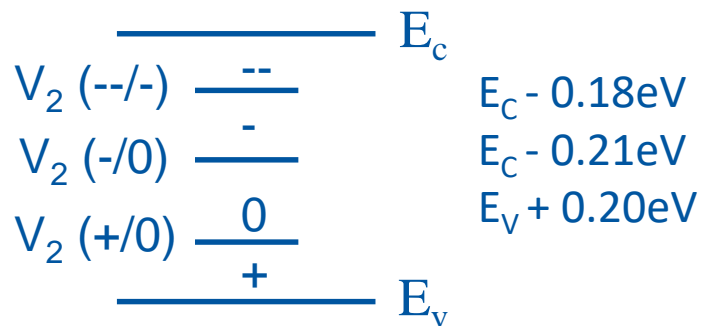


V_2O
two missing silicon atoms
+one oxygen atom



Electrical activity of the V_2

- The divacancy has two acceptor levels in the upper half of the band gap and a donor level in the lower half of the band gap.



Watkins, Corbett: Phys.Rev., 121,4, (1961), 1001

Defect Characterization Techniques

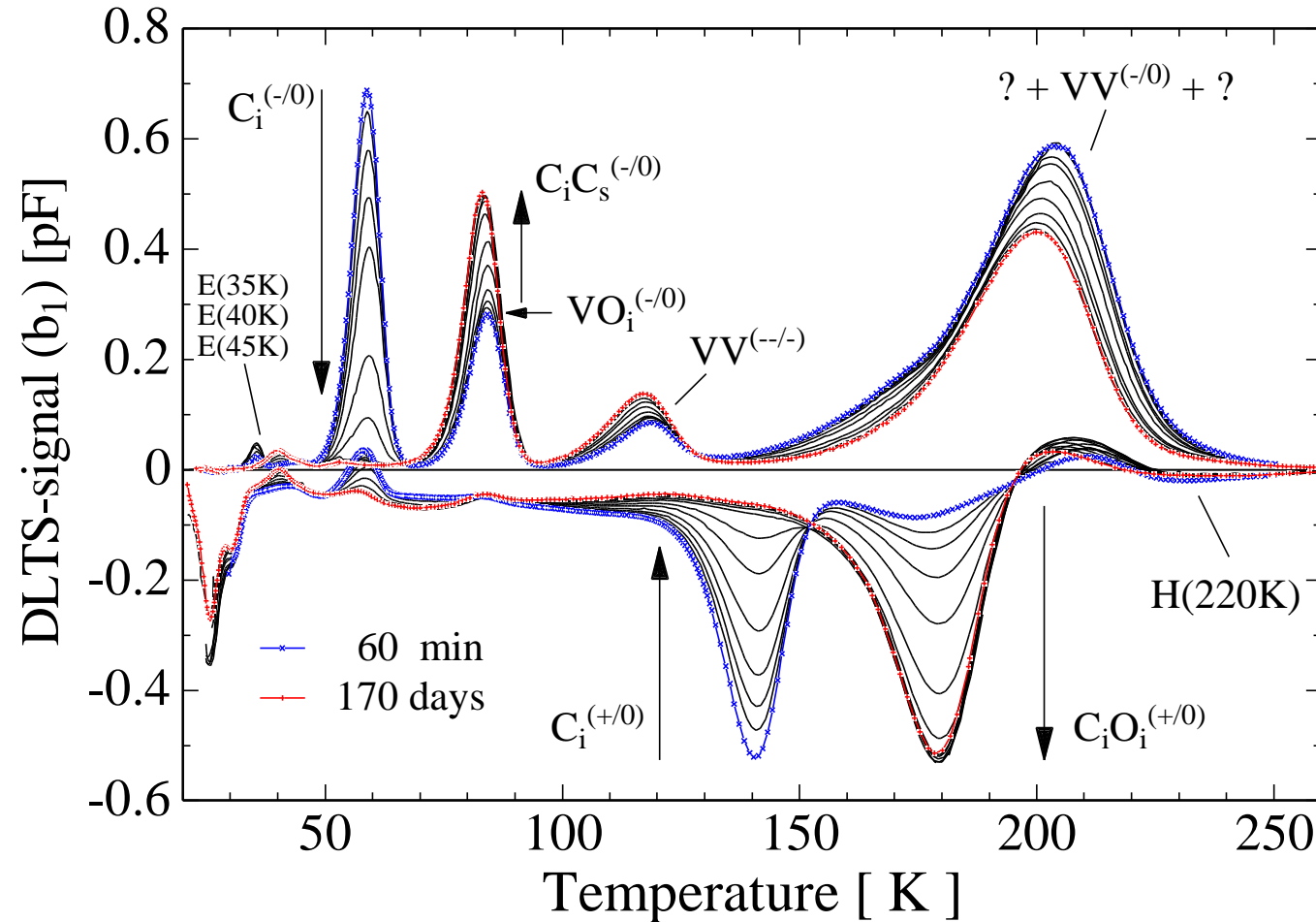
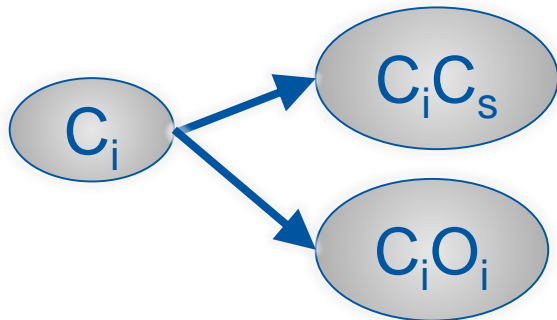
Deep Level Transient Spectroscopy



Example: n-type FZ silicon sensor irradiated with MeV neutrons

DLTS spectra recorded during **annealing** at room temperature

Carbon interstitial (C_i) defect kinetics clearly visible:



- Introduction rates of main defects $\approx 1 \text{ cm}^{-1}$
- Introduction rate of negative space charge $\approx 0.05 \text{ cm}^{-1}$

DLTS (Deep Level Transient Spectroscopy): Operation principle



- Assumption: Defect is an electron trap in n-type silicon, i.e. a majority carrier trap

Measurement cycle at fixed T

[1] reverse bias V_R

- junction under reverse bias
- defect states are not occupied

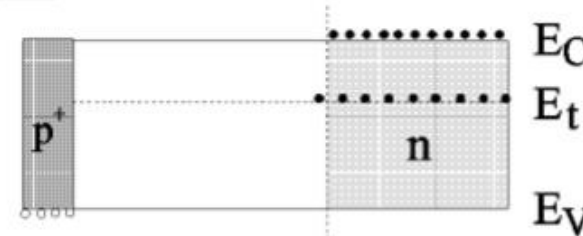
[2] injection pulse V_P

- reduction of reverse bias
- injection of majority carriers
- occupation of defect levels

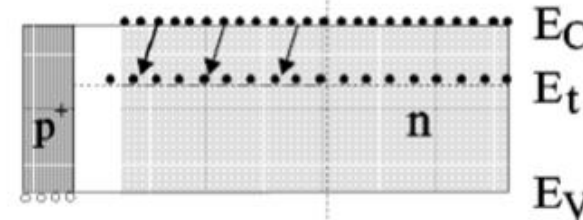
[3] reverse bias V_R

- junction under reverse bias
- thermal emission of carriers
 - expansion of depletion zone
 - decrease of capacitance

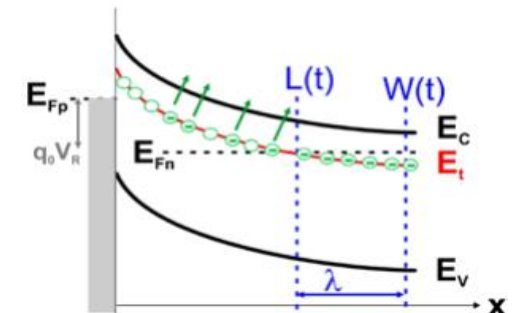
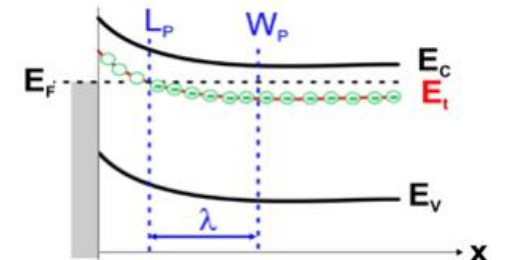
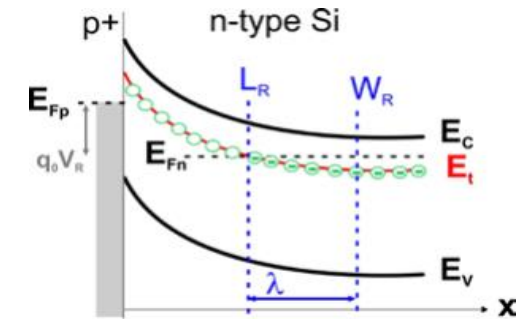
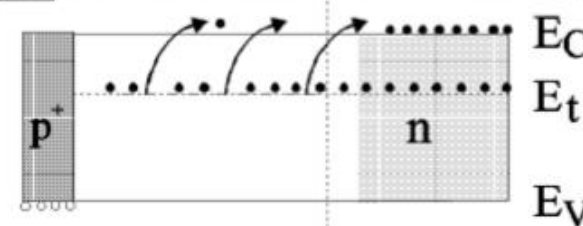
1 Quiescent reverse bias (V_R)



2 Majority carrier pulse (V_P)



3 Thermal emission of carriers (V_R)



DLTS (Deep Level Transient Spectroscopy): Operation principle



Measurement cycle at fixed T

[1] reverse bias V_R

- junction under reverse bias
- defect states are not occupied

[2] injection pulse V_p

- (a) reduction of reverse bias
 - injection of majority carriers

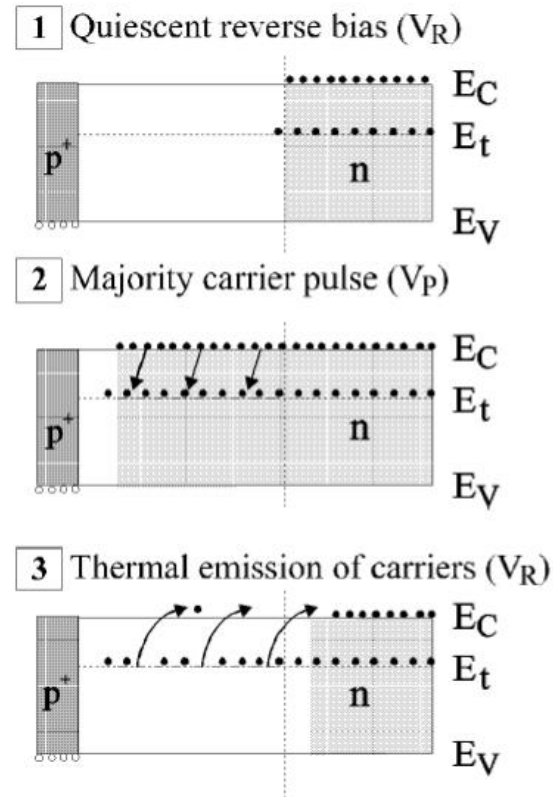
OR

- (b) forward bias
 - injection of minority & majority carriers

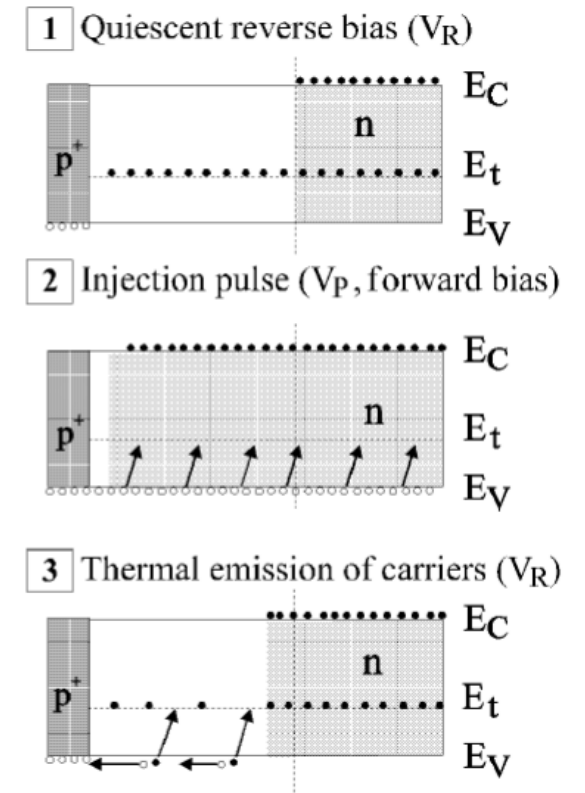
[3] reverse bias V_R

- junction under reverse bias
- thermal emission of carriers
 - expansion of depletion zone
 - change of capacitance

(a) majority carrier injection
(electrons in n-type silicon)
electron trap



(b) high injection ($n \approx p$)
(electrons and holes injected)
hole trap with $c_p \gg c_n$



DLTS (Deep Level Transient Spectroscopy): Operation principle



[3] reverse bias V_R

- junction under reverse bias
- thermal emission of carriers
 - expansion of depletion zone
 - change of capacitance

Change of capacitance:

- trapped carriers change space charge (N_{eff})
- space charge determines depletion depth w
- depletion depth determines the capacitance

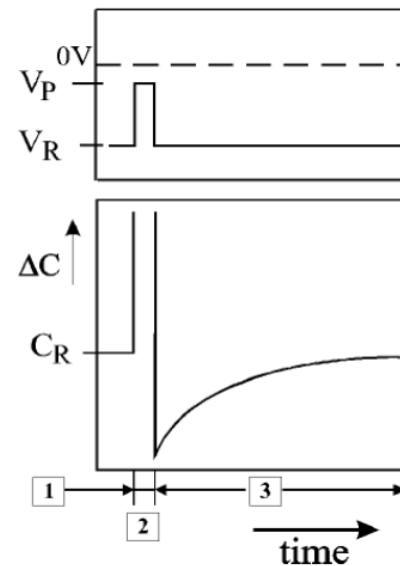
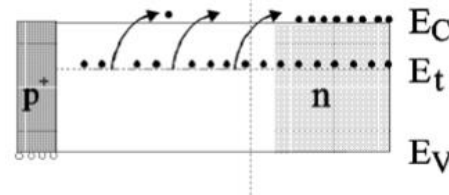
$$C(w) = \epsilon_0 \epsilon_{Si} \frac{A}{w(V)} = A \sqrt{\frac{\epsilon_0 \epsilon_{Si} q_0 |N_{eff}|}{2(V + V_{bi})}}$$

$C(t=0) < C_R$: trapping of majority carriers

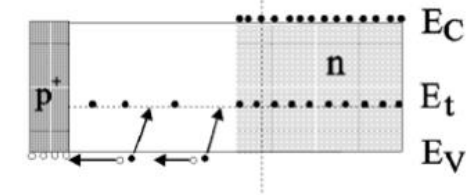
$C(t=0) > C_R$: trapping of minority carriers

sign of ΔC allows to differentiate between electron and hole traps

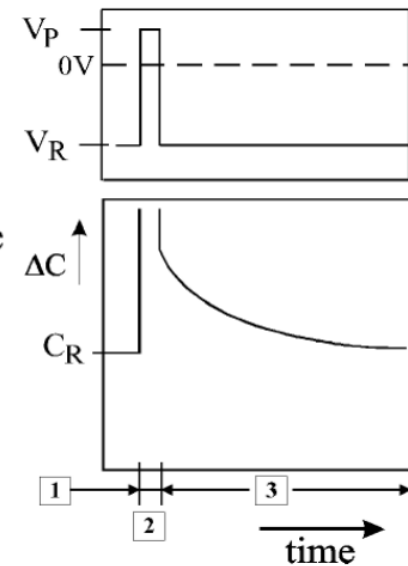
(a) majority carrier injection
(electrons in n-type silicon)
electron trap



(b) high injection ($n \approx p$)
(electrons and holes injected)
hole trap with $c_p \gg c_n$



Bias pulse

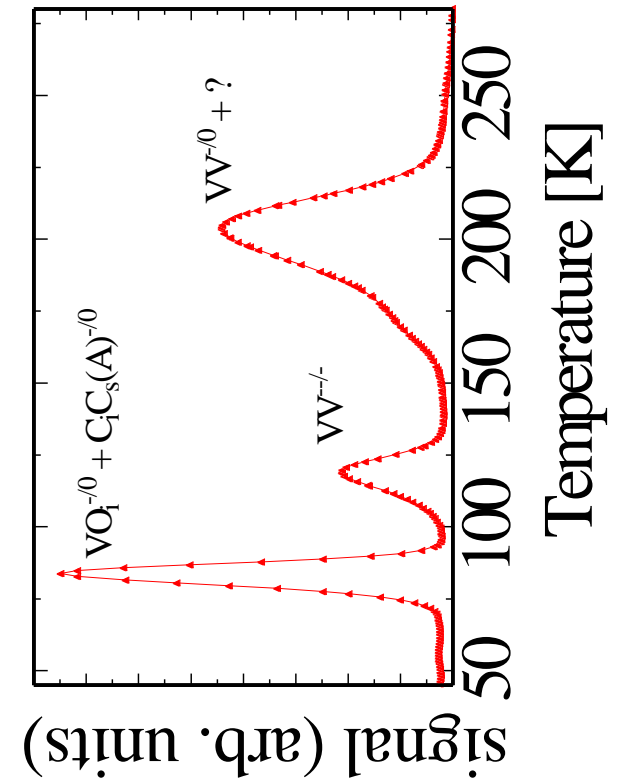
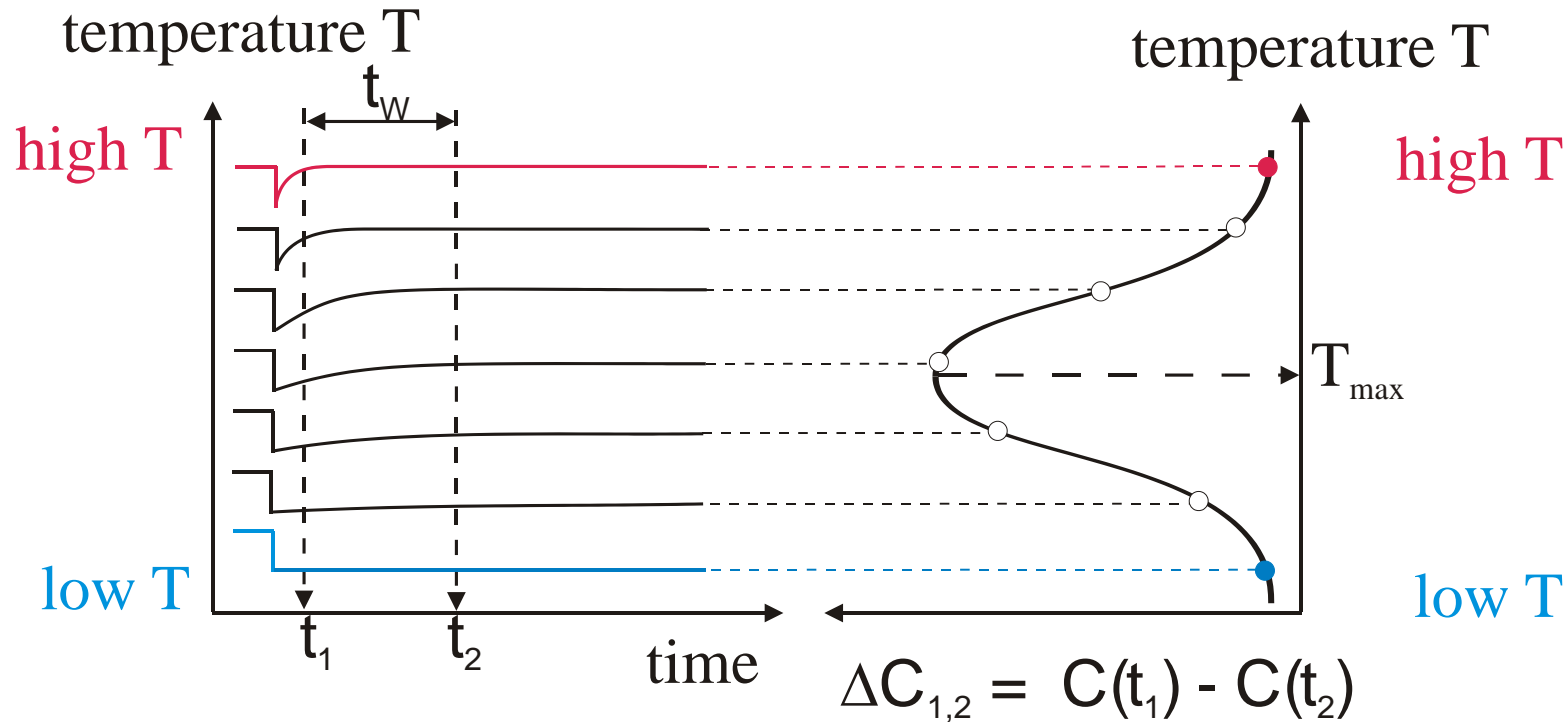


Capacitance transient

DLTS (Deep Level Transient Spectroscopy): Spectrum



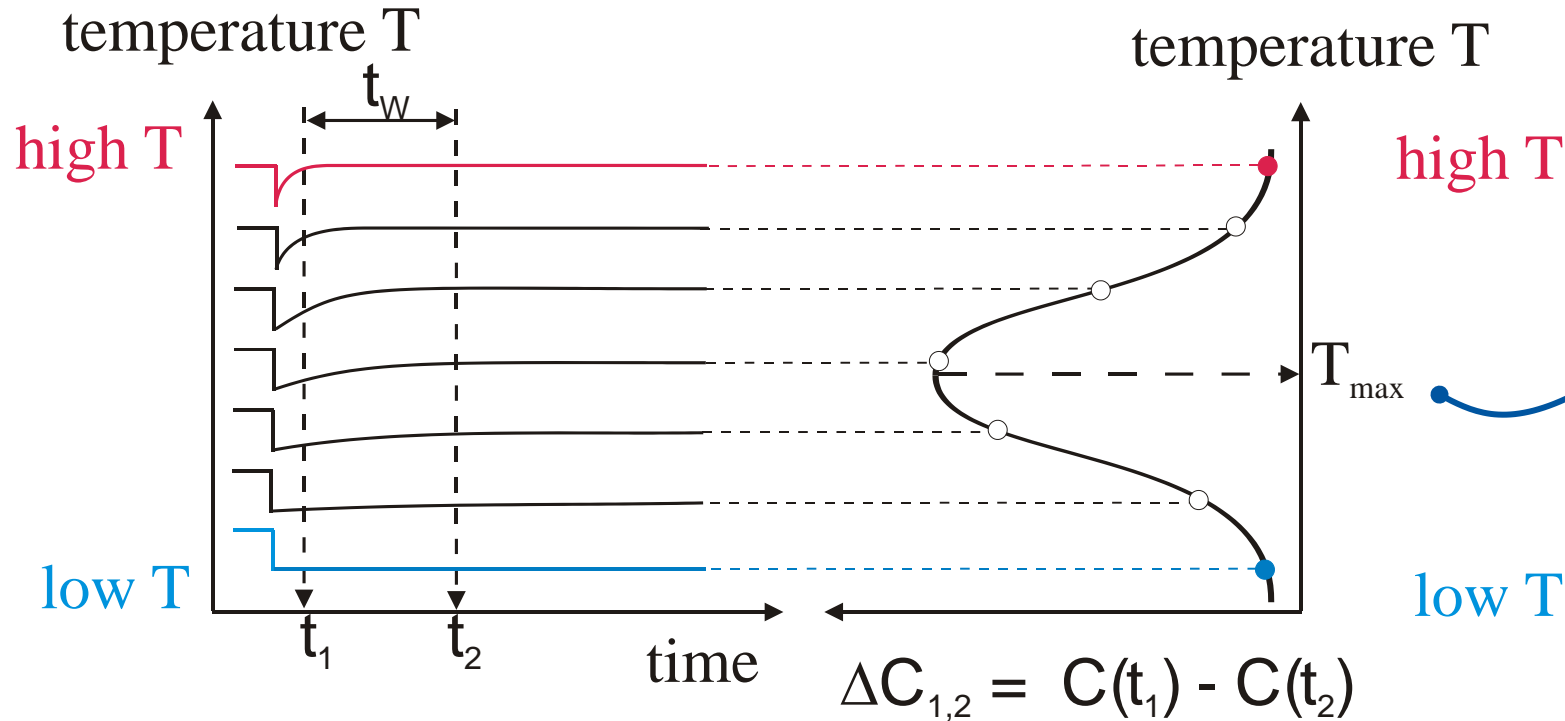
- **DLTS spectrum** is obtained from transients measured at different temperatures



DLTS (Deep Level Transient Spectroscopy): Transient Analyses



• DLTS spectrum



emission time constant at peak maximum temperature can be extracted from time window parameters

$$\tau_e(T_{max}) = \frac{t_2 - t_1}{\ln\left(\frac{t_1}{t_2}\right)}$$

perform several measurements with different time windows to gain a set of $\tau_e(T_i)$, T_i pairs and use them to construct an **Arrhenius Plot**

Transient Analyses: Defect parameters from Arrhenius Plot



Emission rate

$$e_{n,p} = \frac{1}{\tau_e} = \sigma_{n,p} \cdot v_{th,n,p} \cdot N_{C,V} \cdot \exp\left(-\frac{E_a}{k_B T}\right)$$



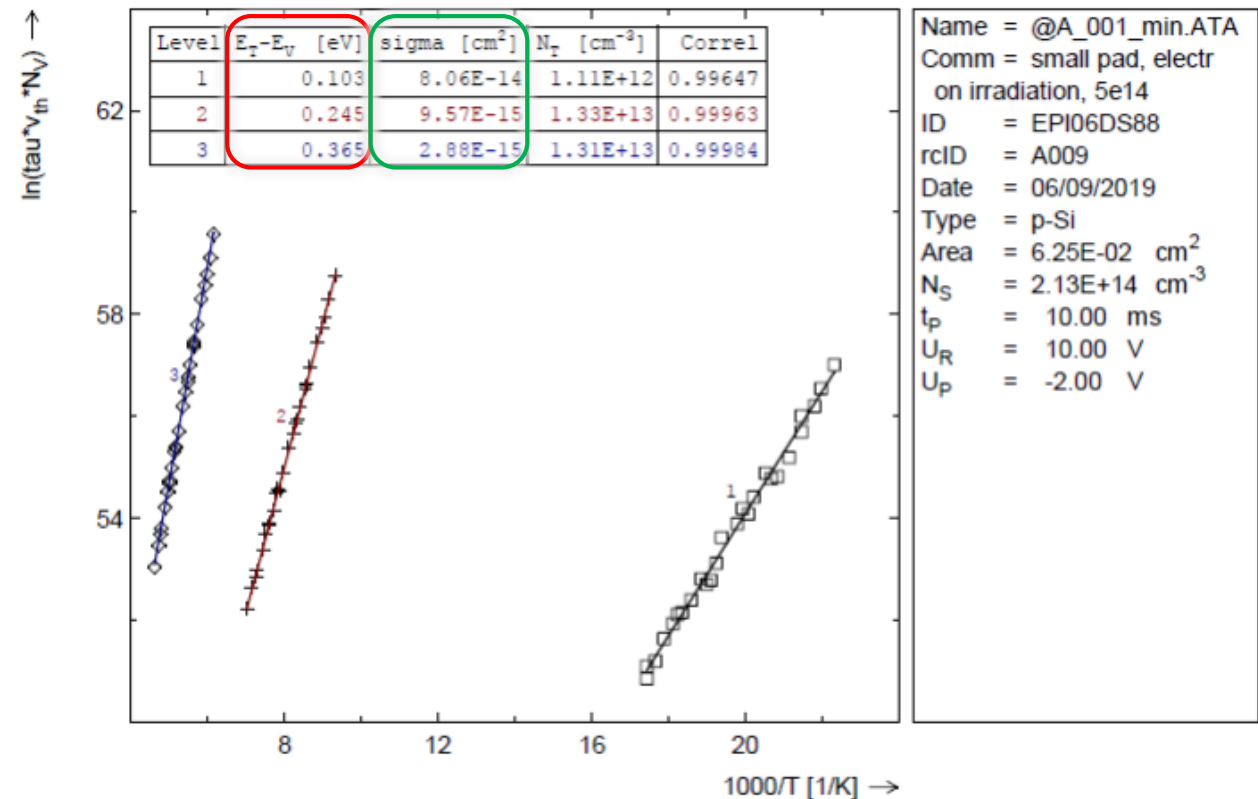
Arrhenius Plot

$$\ln(\tau_e v_{th,n,p} N_{C,V}) = -\ln(\sigma_{n,p}) + \frac{E_a}{k_B T}$$

- e_n emission rate electrons
- τ_e emission time constant
- c_n capture coefficient electrons ($c_n = \sigma_n v_{th,n}$)
- σ_n capture cross section for electrons
- v_{th} thermal velocity
- N_C density of states in conduction band
- k_B Boltzmann constant

Defect parameters extracted from Arrhenius plot

- slope: **activation energy E_a**
- intercept: **capture cross section σ**



DLTS (Deep Level Transient Spectroscopy): Transient Analyses



• Various signal processing techniques

• Analog signal processing

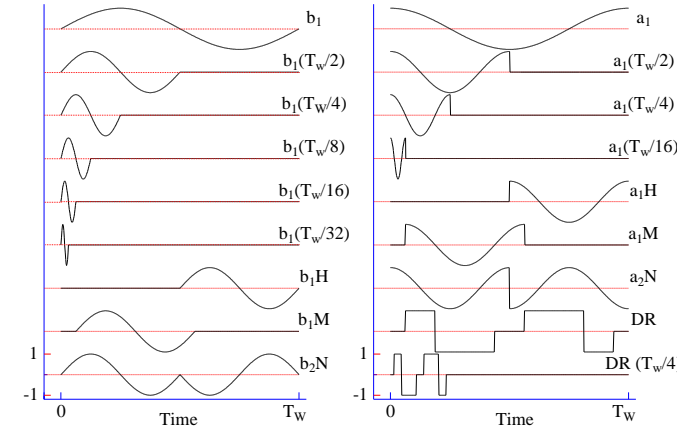
- double boxcar integrator
- lock-in amplifier, analog correlator,

• Digital signal processing

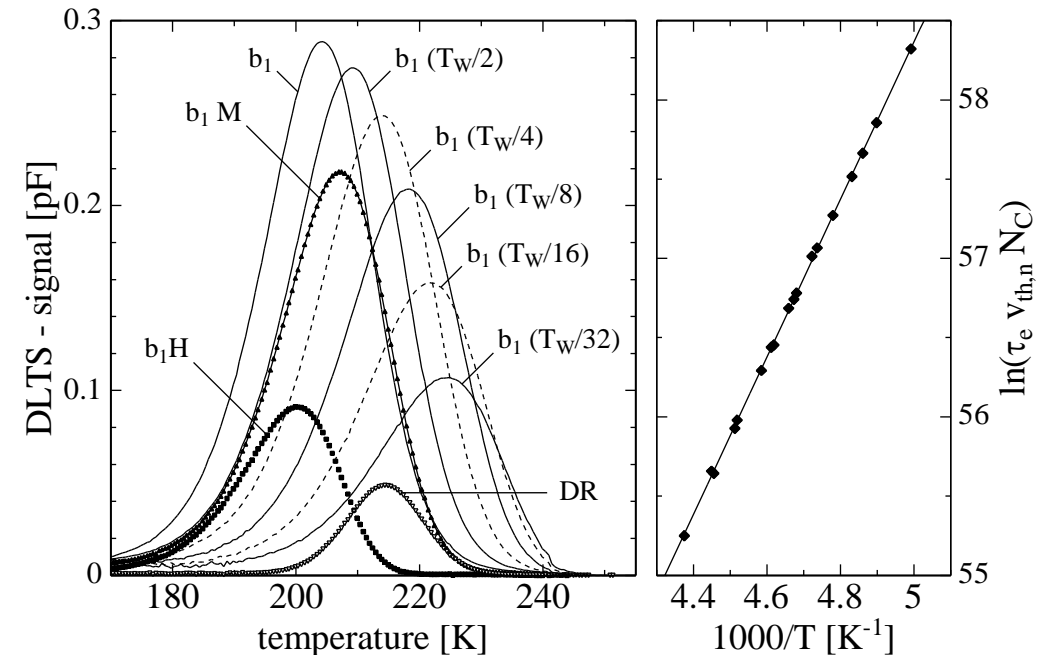
- Fast-Fourier Transformation FFT
- Laplace Transformation
- Various correlator functions
- ..

Example used at CERN:

- Folding transient with 28 different correlator functions
- maxima analysis of a single DLTS scan (one time window) leads to 28 value pairs (τ_e, T) which can be used for an Arrhenius plot



correlator functions



DLTS: Determination of Defect Concentration

- Band bending diagrams for deep acceptor:

[2] during filling pulse

[3] during transient phase

- Transition region λ :
$$\lambda = \sqrt{\frac{2\epsilon\epsilon_0(E_F - E_t)}{q_0^2 N_D}}$$

- Defect concentration N_t

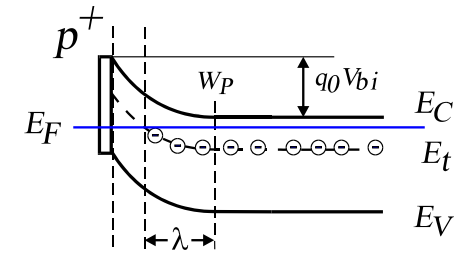
- Amplitude of the C-transient $\Delta C_0 \sim N_t$

$$N_t = -2N_D \frac{\Delta C_0}{C_R} \left[1 - \left(\frac{C_R}{C_P} \right)^2 - \frac{2\lambda C_R}{\epsilon\epsilon_0 A} \left(1 - \frac{C_R}{C_P} \right) \right]^{-1}$$

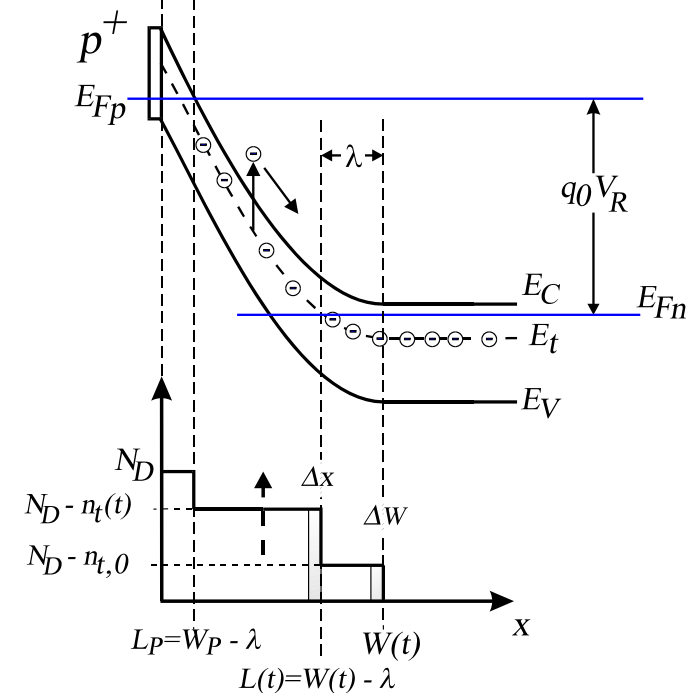
- For $\lambda \ll W_R$ simplifies to:

$$N_t \approx 2N_D \frac{|\Delta C_0|}{C_R}$$

Filling pulse: $V_p = 0V$ (2)



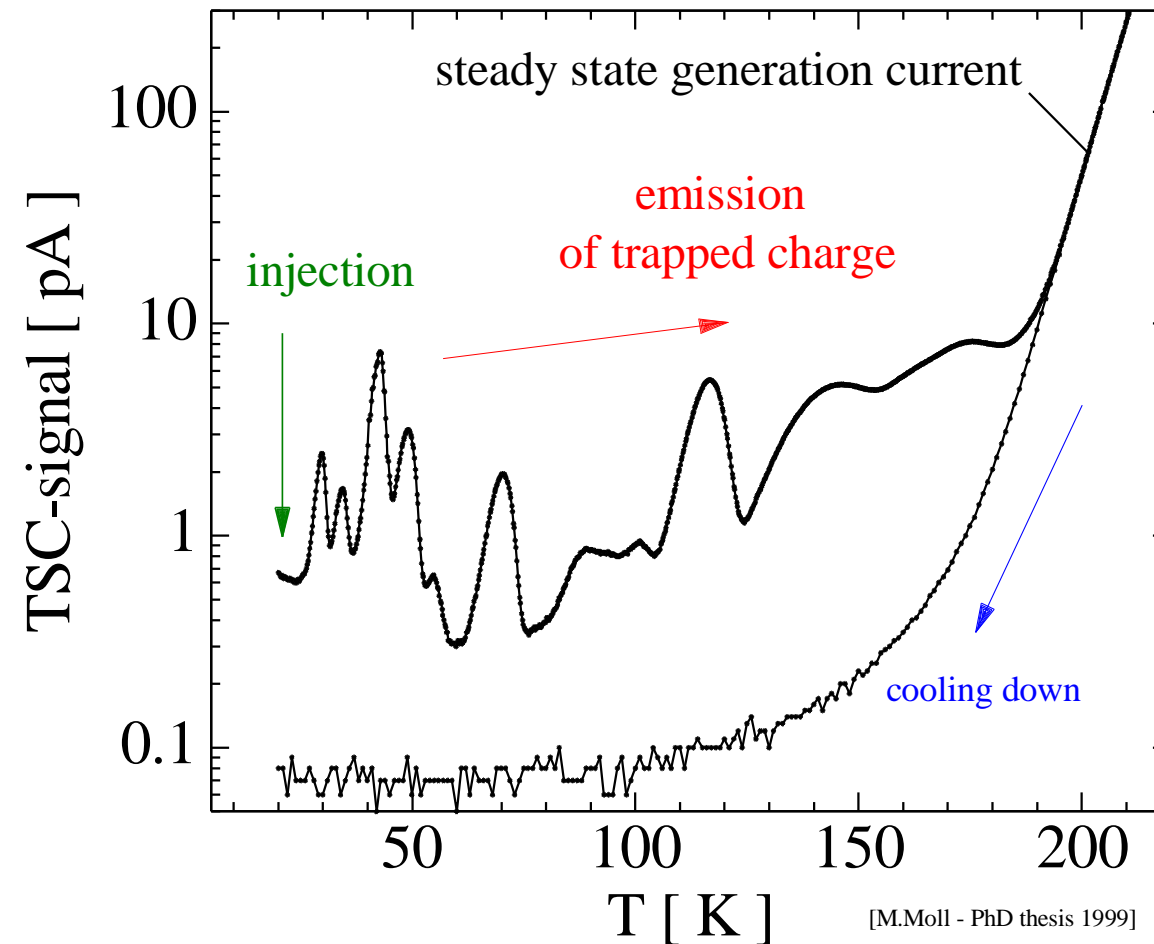
Transient: Reverse bias V_R (3)



TSC: Thermally Stimulated Current



- Measurement cycle
 - (1) **Cooling**
 - under bias or without
 - (2) **Filling (charge injection)**
 - Forward bias, zero bias, optical filling
 - (3) **Current measurement**
 - Measure current while ramping up the temperature, discharging of traps results in current peaks
- Analyses
 - **Peak heights** or integral over peak
 - → Defect concentration
 - **Peak position** gives indication for E_a and cross section σ
 - more precise: fit to spectrum and/or delayed heating measurement (see next slide)



[M.Moll - PhD thesis 1999]

Current

$$I_{TSC}(T) = \frac{1}{2} q_0 A w(T) N_t \cdot e_n(T) \cdot \exp\left(-\frac{1}{\beta} \int_{T_0}^T e_n(T) dT\right)$$

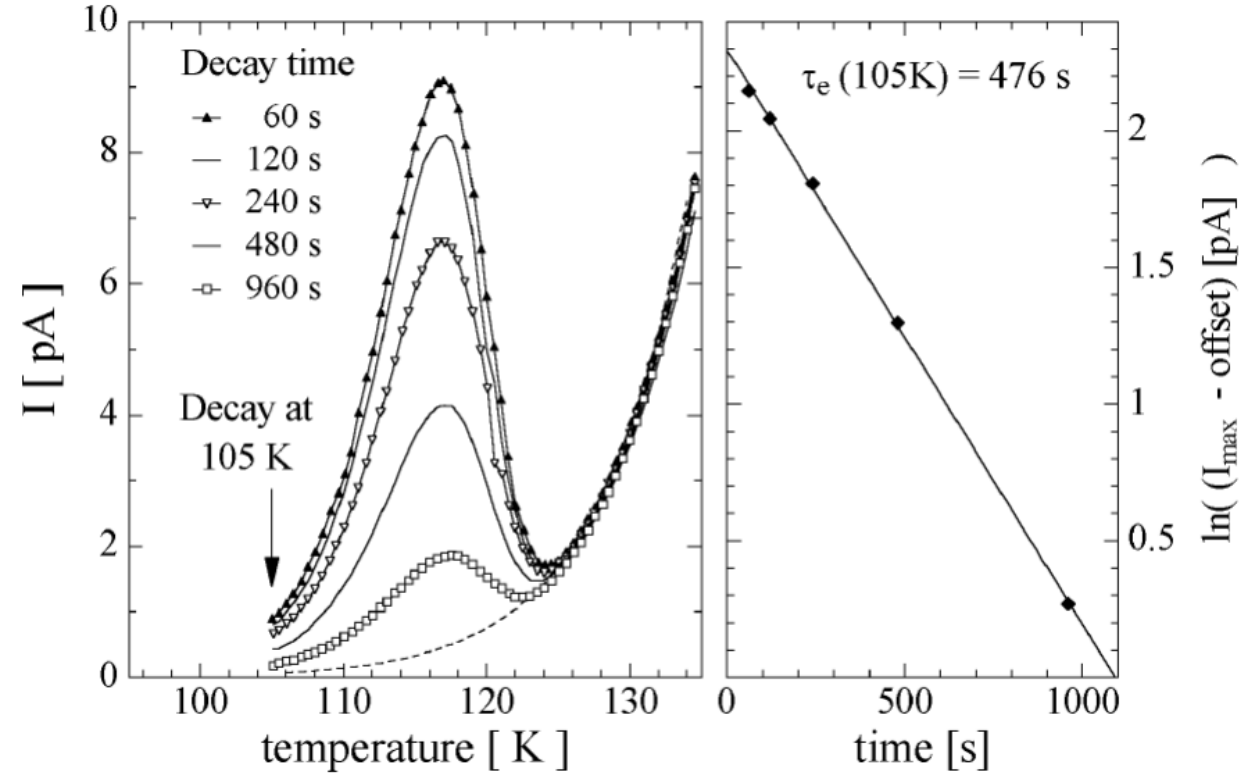
Note: hole and electron traps give same polarity signal

TSC: Delayed heating method



- “Delayed heating” or “Thermal cleaning”

- Measuring the TSC peak several times with different delay times between the end of filling at T_0 and the start of heating
- **Increasing delay time:** more charge carriers already emitted at $T_0 \rightarrow$ TSC peak decreases
- **Plot** logarithm of the peak amplitude against delay time \rightarrow slope: emission time constant $\tau_e(T_0)$
- Repeat the delay measurements at different T_0
 \rightarrow Arrhenius-plot to determine E_a and σ

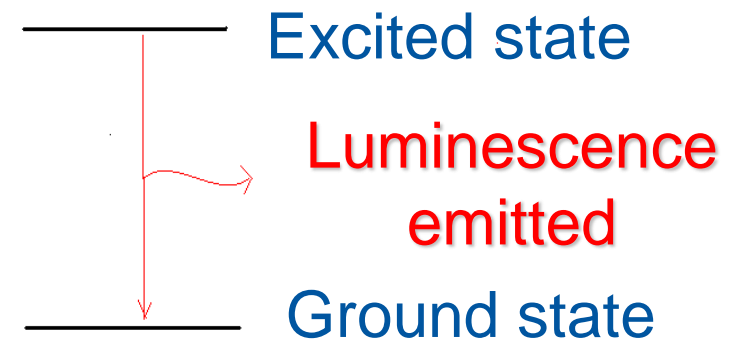
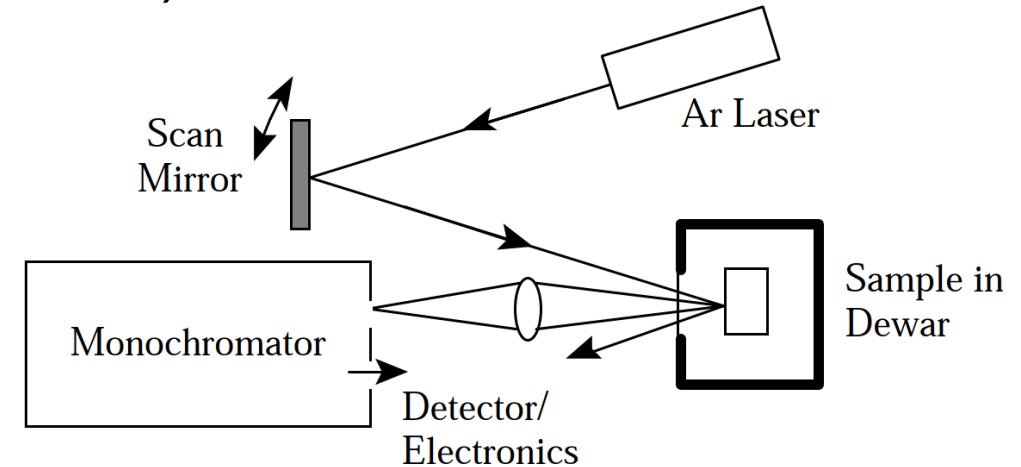


Photoluminescence (PL) [1/2]



Excitation of the sample with light ('photo') and re-emission of part of the absorbed energy as light ('luminescence')

- Excitation is usually by a laser, for convenience of directed beam, with beam power of 100's of mW.
- Green laser light is absorbed by the crystal, exciting an electron from the valence band to the conduction band, with a penetration depth of $1/e = 1 \mu\text{m}$.
- Electron-hole pairs (excitons) are created with a lifetime of 10's of ms in pure Si.
 - Excitons are captured by impurities, exciting the impurity.



Photoluminescence (PL) [2/2]

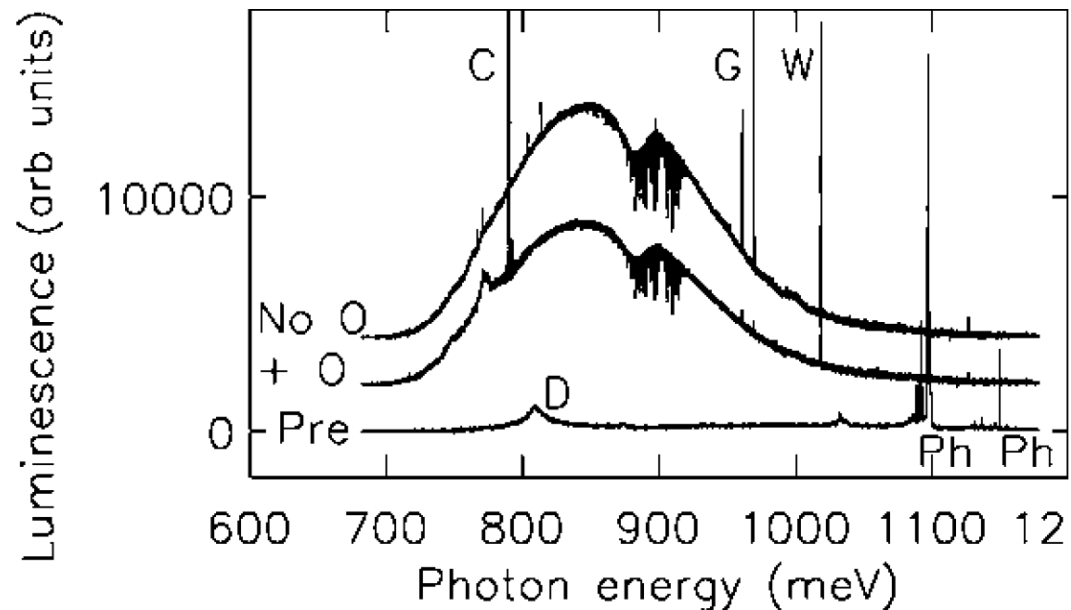


- **What is observed?**

- Only (usually) neutral centres (not charged)
- Required concentrations for detection are over 10^{11} cm^{-3} ; best 10^{14} to 10^{16} cm^{-3}
- Very sharp lines with typical energy resolution of 0.1 meV
- PL is not a quantitative method: PL not necessarily proportional to the concentration of defect

- **Example:**

- Standard FZ silicon (No O)
- Oxygenated FZ silicon (+O)
- irradiated with 23 GeV protons
 - fluence 10^{16} cm^{-2}



C-line: C_iO_i
G-line: C_iC_s
W-line: Si_i related

Phosphorus
(before irradiation)

Infrared Spectroscopy (FTIR) [1/3]

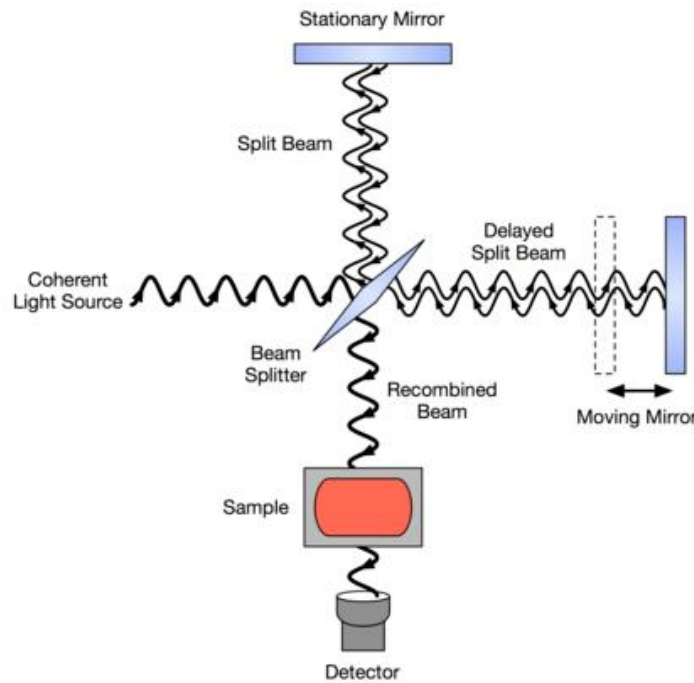


- Measurement of the light transmitted through a sample thickness d with polished parallel surfaces

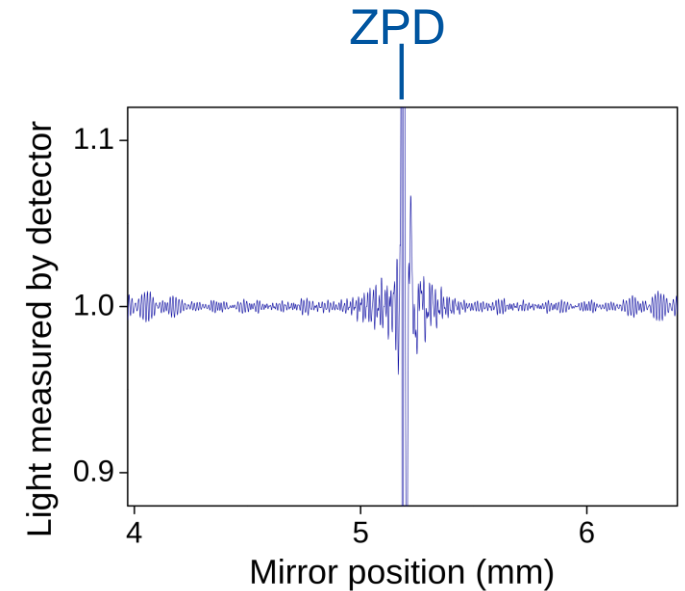
$$I = I_0 \frac{(1 - R)^2 \exp(-\alpha d)}{1 - R^2 \exp(-2\alpha d)}$$

I_0 light intensity incident on the sample
 d thickness of the sample
 α frequency dependent absorption coefficient
 R reflectivity

$$R \approx \left[\frac{n - 1}{n + 1} \right]^2 \approx 0.3 \text{ in the mid infrared}$$



Michelson Interferometer

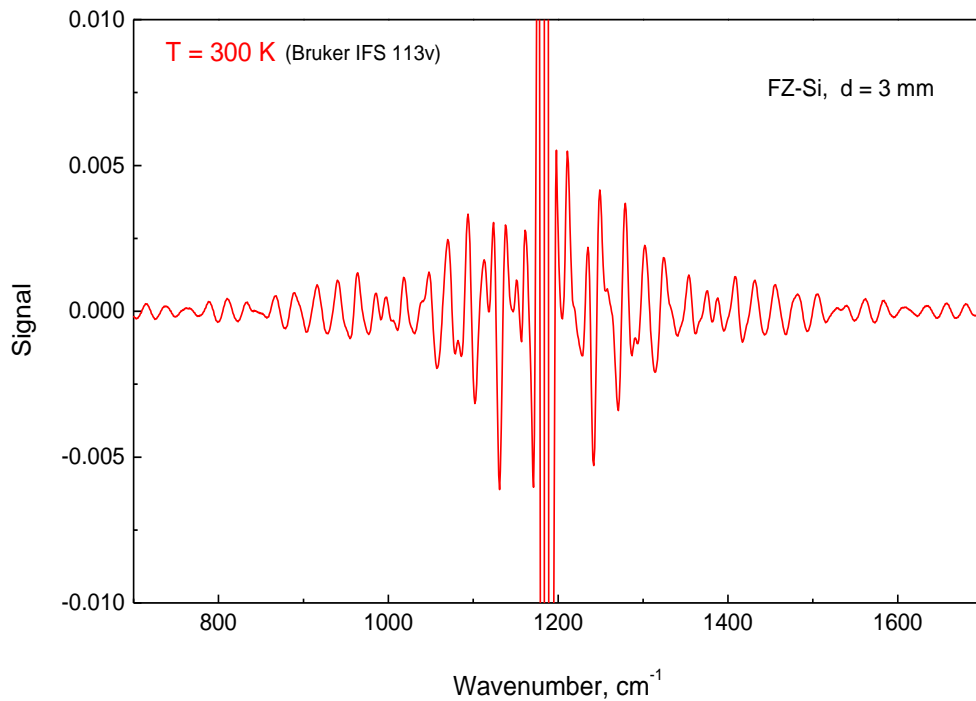


Interferogram

Infrared Spectroscopy (FTIR) [2/3]

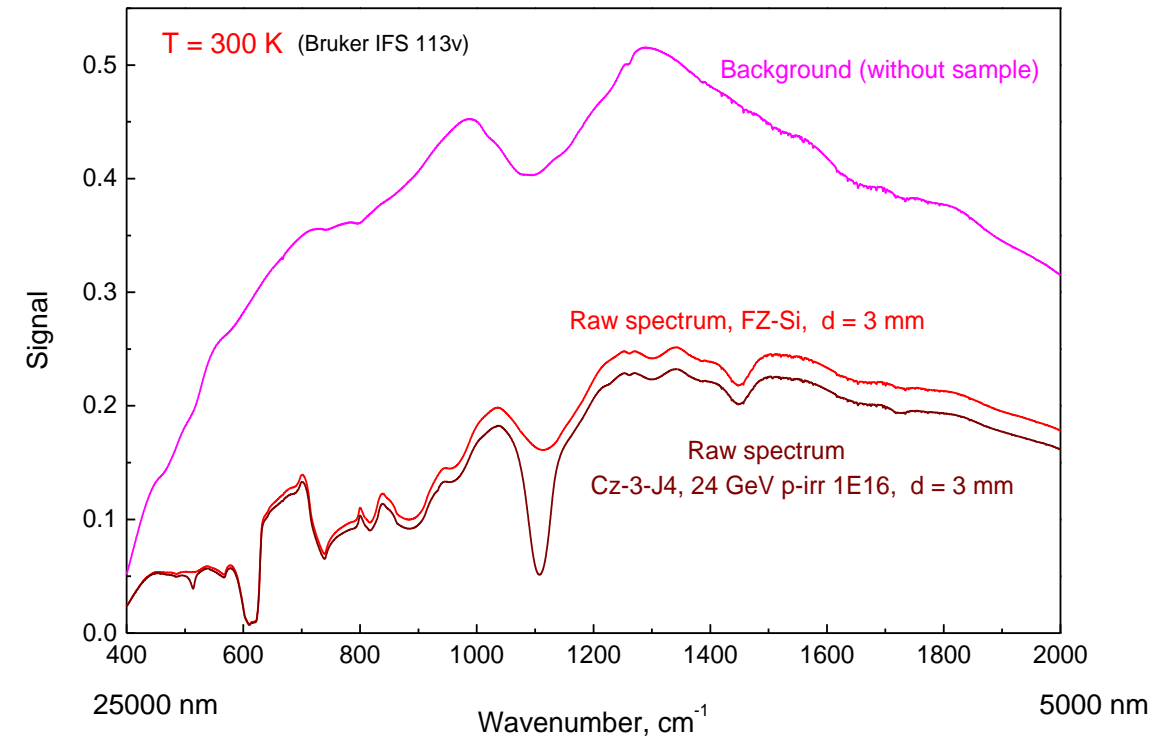


- FTIR – Fourier Transform Infrared Spectroscopy



Interferogram

Fourier Transformation

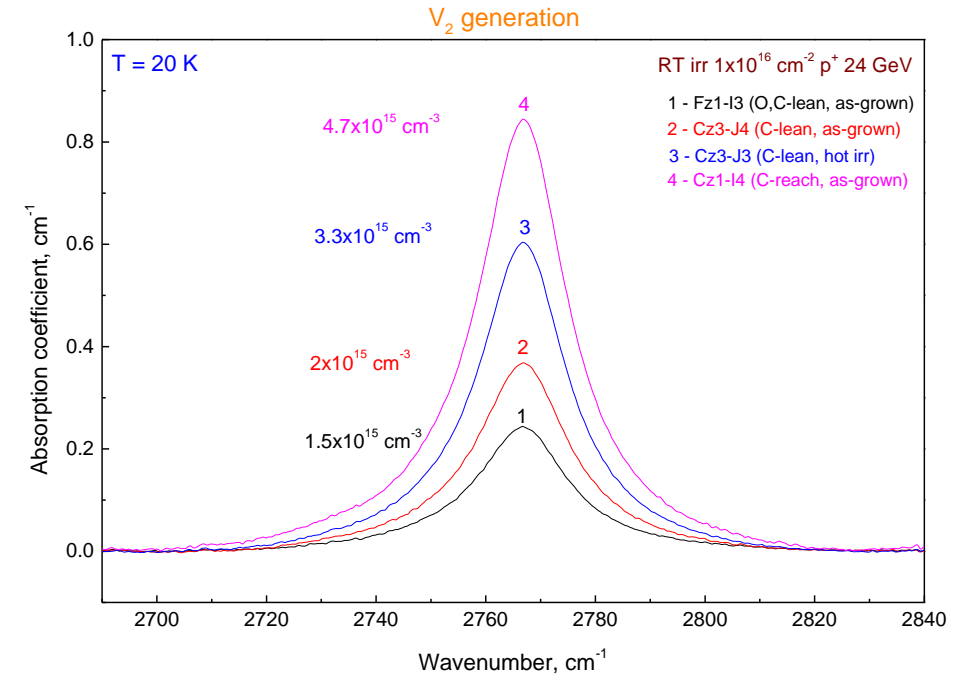
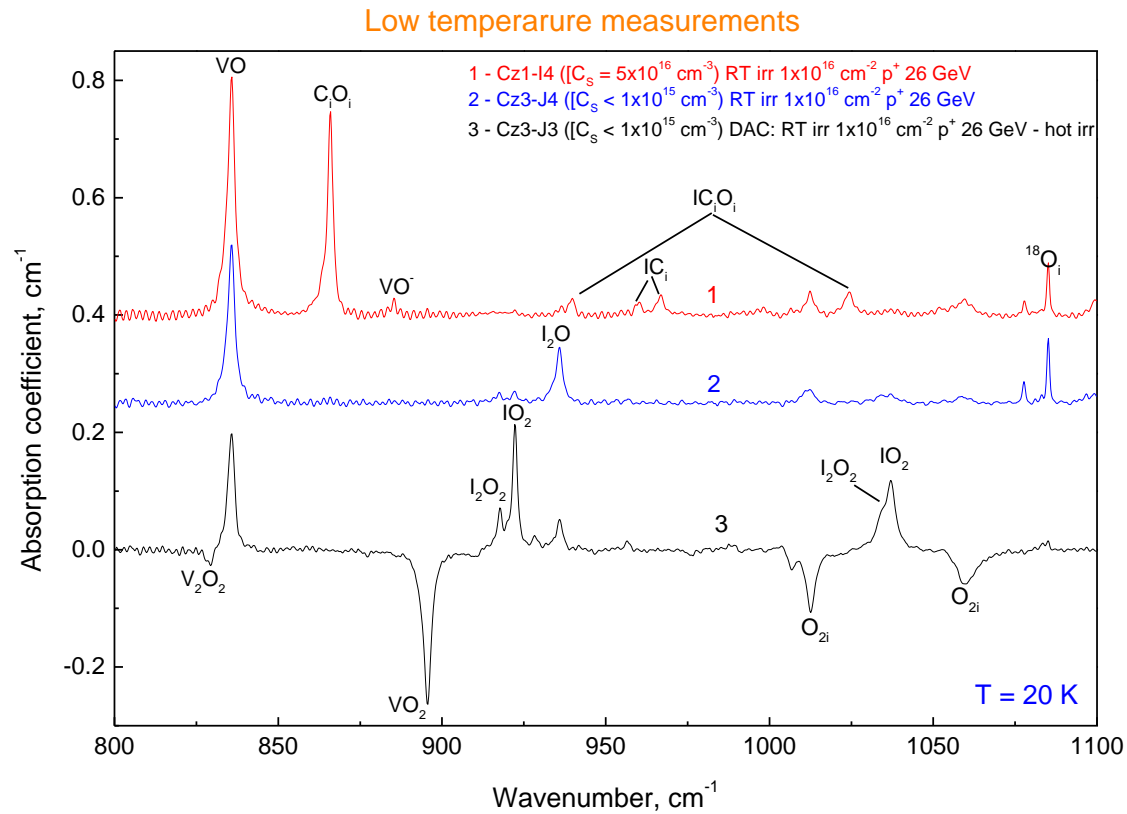


Spectrum

Infrared Spectroscopy (FTIR) [3/3]



• Measurements at low temperature (20K)

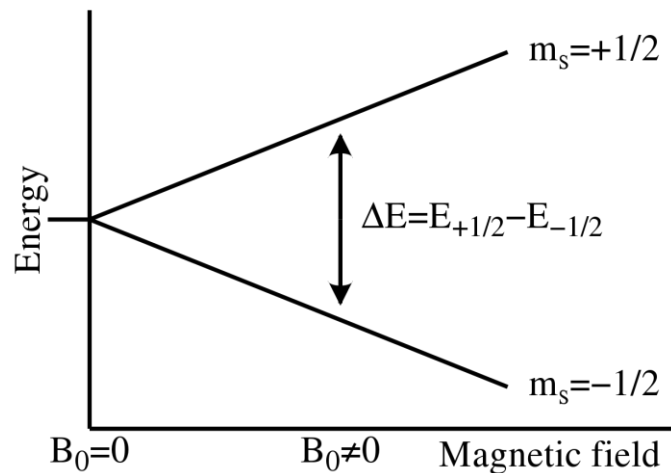


- Detection limits depend on
 - measurement temperature (LT or RT)
 - Sharpness of the lines
 - Wavenumber position
- Detection limits normally in the range
 - 5×10^{13} to 10^{15} cm^{-3}

EPR: Electron Paramagnetic Resonance [1/3]

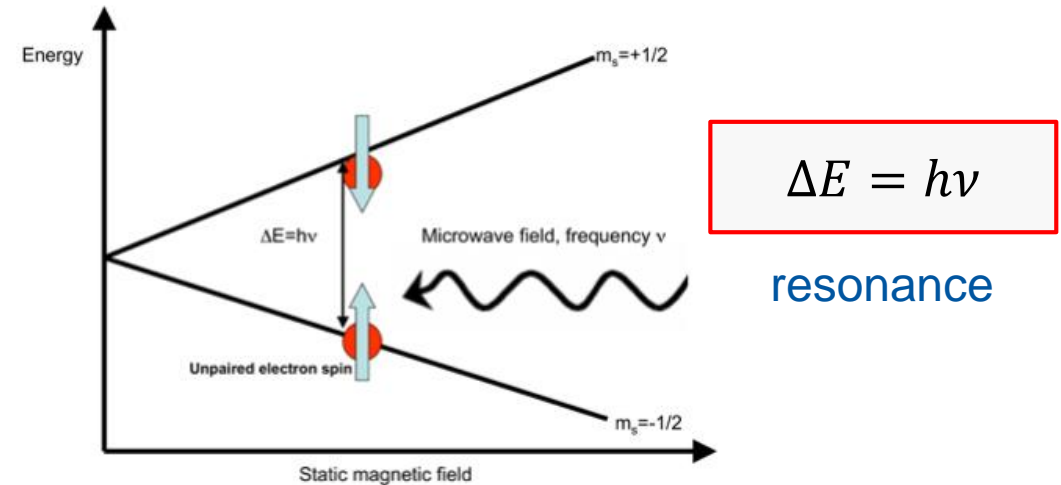


- **EPR** is the best experimental technique for determining the structure of irradiation induced paramagnetic point defects in semiconductors.
- **EPR** spectroscopy deals with the interaction of the electron spins with external magnetic fields
 - **EPR = Zeeman spectroscopy:** The effect of splitting a spectral line into several components in the presence of a static magnetic field ($B \neq 0$) of defects with unpaired electron states ($S = 1/2, 1, \dots$).



$$\Delta E = g_e \mu_B B_0$$

splitting of energy levels



g_e electron's g-factor
 $g_e = 2.0023$ (free electron)
 μ_B Bohr magneton

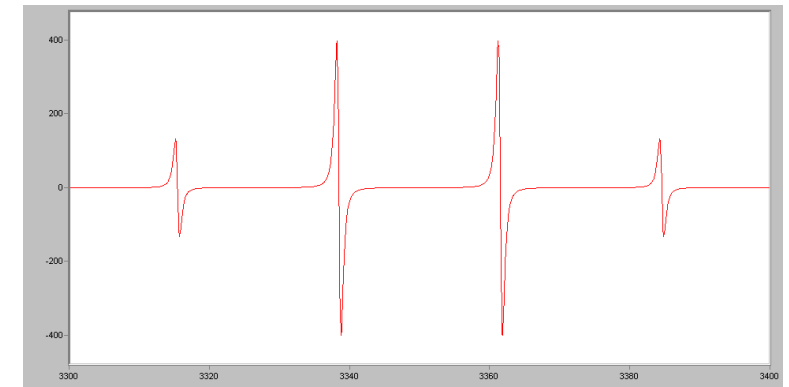
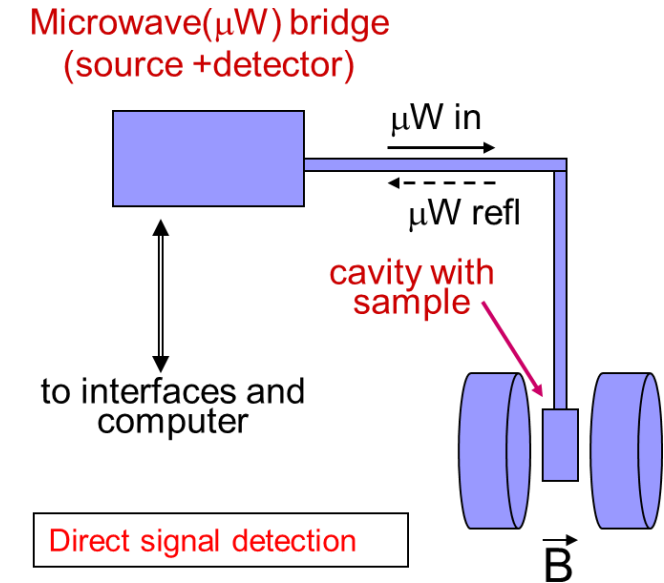
$$1 \text{ Gauss} = 10^{-4} \text{ Tesla} \quad \mu_B = \frac{e\hbar}{2mc}$$

- **The condition of resonance:** $h\nu = \Delta E = g_e \mu_B B_0$, $g_e = 2.0023$ for free electron
 - $\nu \rightarrow 9.5 - 34 \text{ GHz}, 95 \text{ GHz}, \dots$
 - Sensitivity: 2×10^{10} spins/Gauss (~ 1 ppb)

EPR: Electron Paramagnetic Resonance [2/3]



- An unpaired electron can gain or lose angular momentum
 - change the g-factor value through **spin-orbit coupling**
 - **information about the nature of the atomic/molecular orbital containing the unpaired electron - defect 's electronic structure**
 - The magnetic moment of a nucleus ($I \neq 0$) affects any unpaired electrons associated with that atom.
 - **hyperfine splitting** of the EPR resonance signal into doublets, triplets
 - further surrounding nuclei lead to super hyperfine splitting
 - Also the nuclear quadrupole moment impacts on the measured signal
- The g-factor and hyperfine coupling in an atom/ molecule may not be the same for all orientations of the unpaired electron in external magnetic field
 - spectra anisotropy depending on the electronic structure of the atom/molecule
 - → reflects the local structure



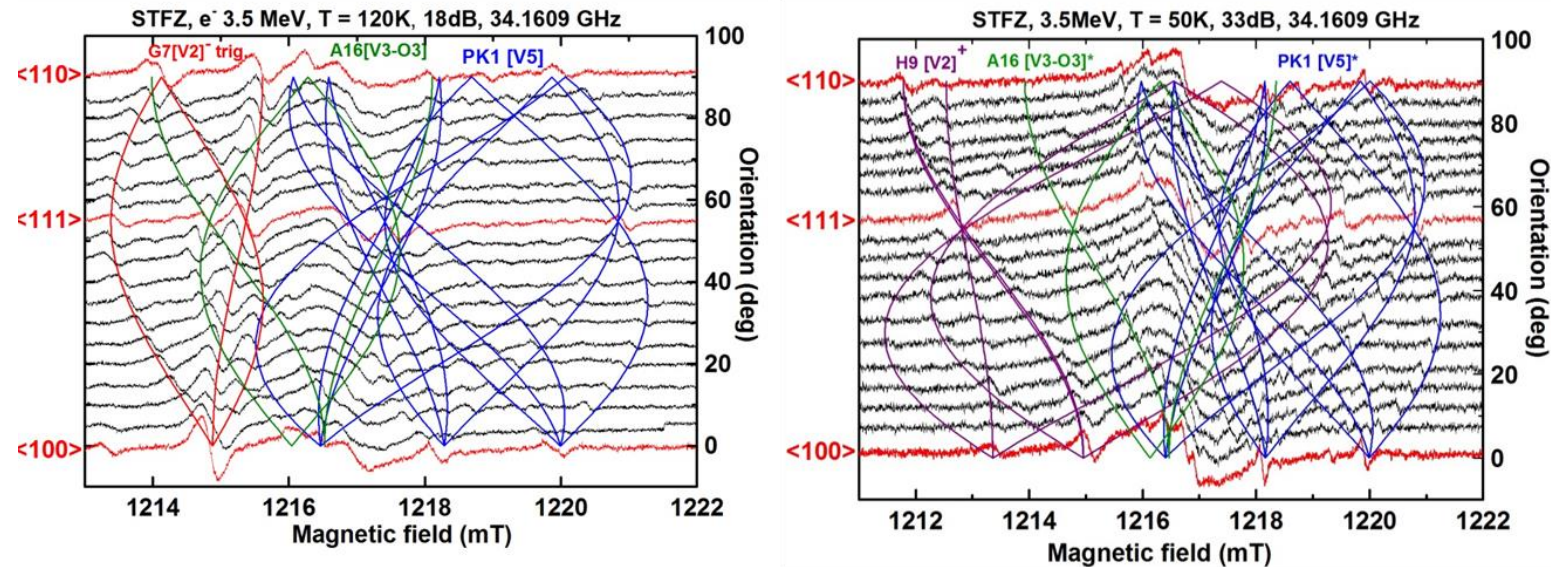
EPR spectrum of CH_3 radical

EPR: Electron Paramagnetic Resonance [3/3]



- Example: EPR results after irradi. with 3.5 MeV electrons, $\Phi=10^{17}$ cm⁻²

Variation of ESR spectra with measuring temperature (120K) and (50 K).



- G7[V2]⁻ (trig.)
- PK1 [V5]^{*} (triclinic) vacancy aggregate seen at 120K.
- A16[V3-O3] (ortorh.)

- G7[V2]⁻ is not observed (ESR signal saturates) at T = 50K.
 - H9 [V2]⁺ (monocl.) observed at T = 50 K.
 - A16[V3-O3]^{*}
 - PK1[V5]^{*}
- } -observed at low μ W power (33 dB).

Radiation Damage

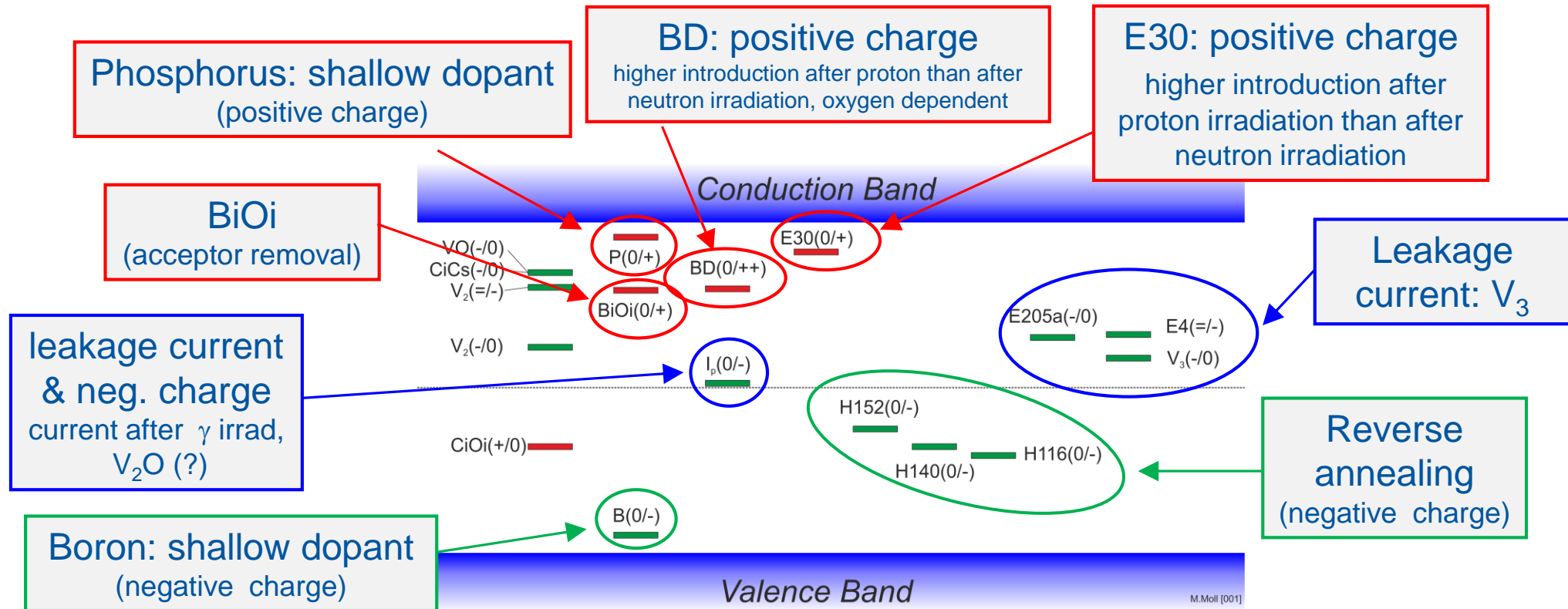
Microscopic Defects vs. Macroscopic Device Properties

Some selected examples with clear correlations between defects and device degradation:

- Leakage current after hadron irradiation (short term annealing)
- Space charge changes during reverse annealing (long term annealing)
- Oxygen enriched silicon: proton vs. neutron damage
- Acceptor removal effect in LGAD sensors

Radiation induced defects with impact on device performance

RD50 map of most relevant defects for device performance near room temperature:

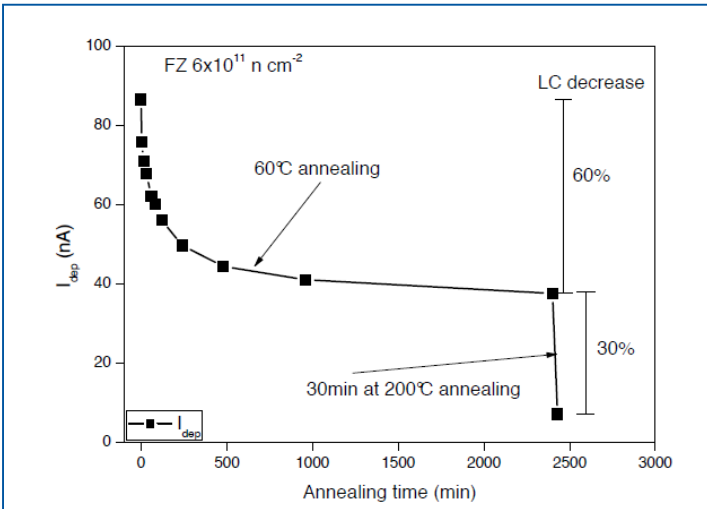


- Trapping: Indications that E205a and H152K are important (further work needed)
- Converging on consistent set of defects observed after p, π , n, γ and e irradiation.
- Defect introduction rates are depending on particle type and energy, and some on material!

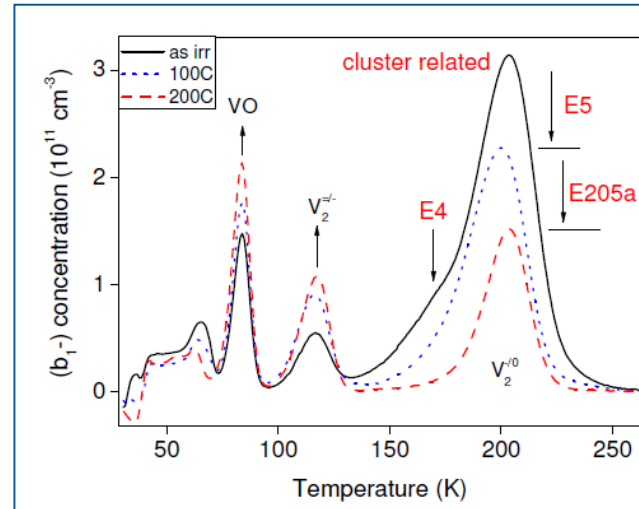
Example: Defects with impact on leakage current



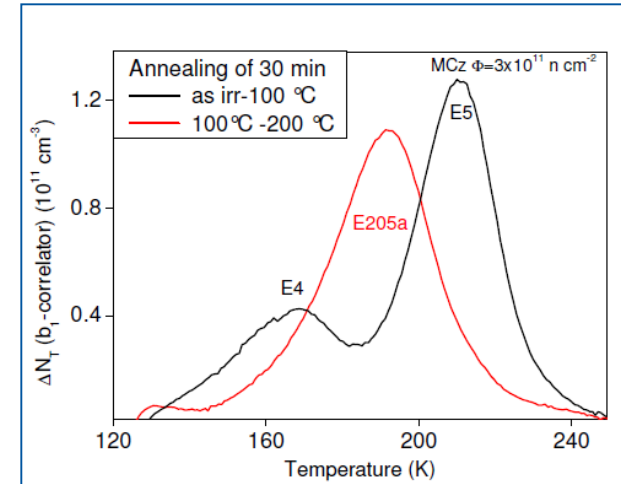
- Macroscopic observation: Leakage current build-up following NIEL (for hadrons)
 - Leakage current scaling (almost) with NIEL and independent of silicon material (not for gammas!)
 - Leakage current is annealing in time and with temperature.
- Example: Annealing study on a FZ sample ($6 \times 10^{11} \text{ n/cm}^2$)



Leakage Current

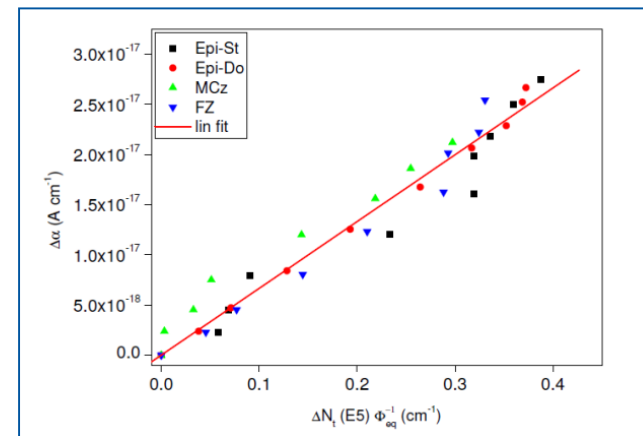


DLTS spectra



DLTS difference spectra (disappearing peaks)

- Microscopic observation:
 - The defects E4/E5 (annealing at 60°C) and E205a (annealing at 200°C) are contributing to the leakage current with 60% and 30 % respectively.



Decrease in defect concentration

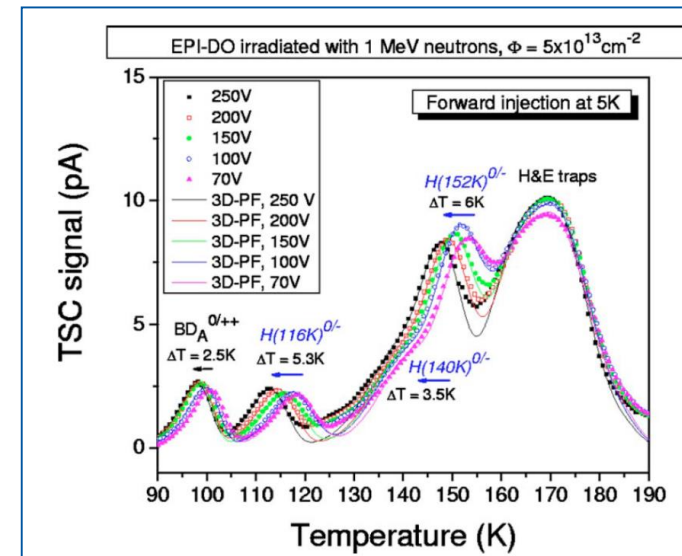
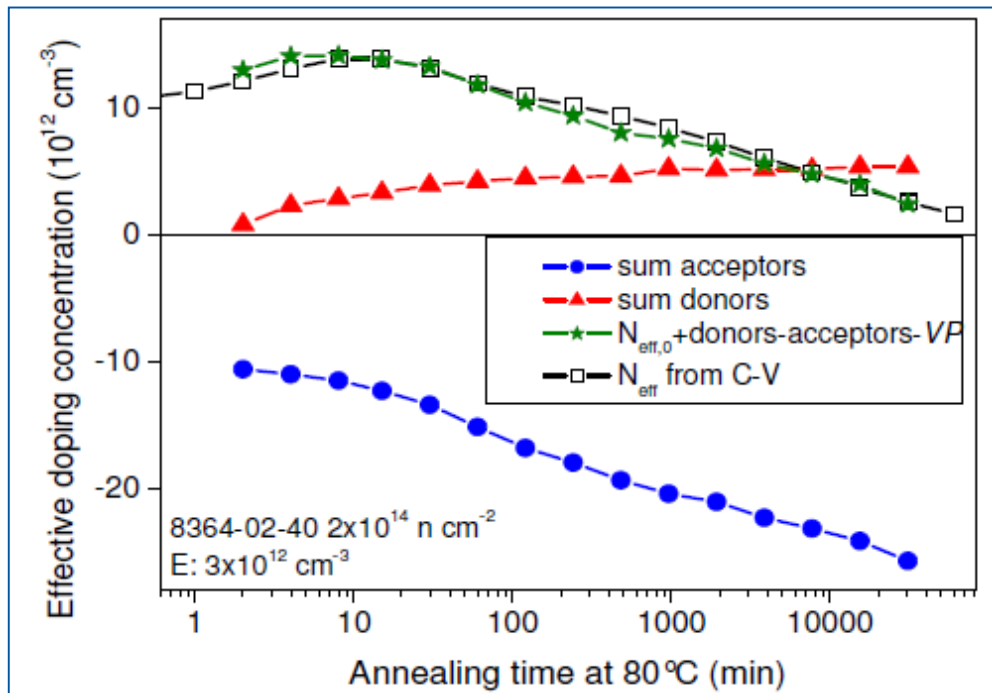
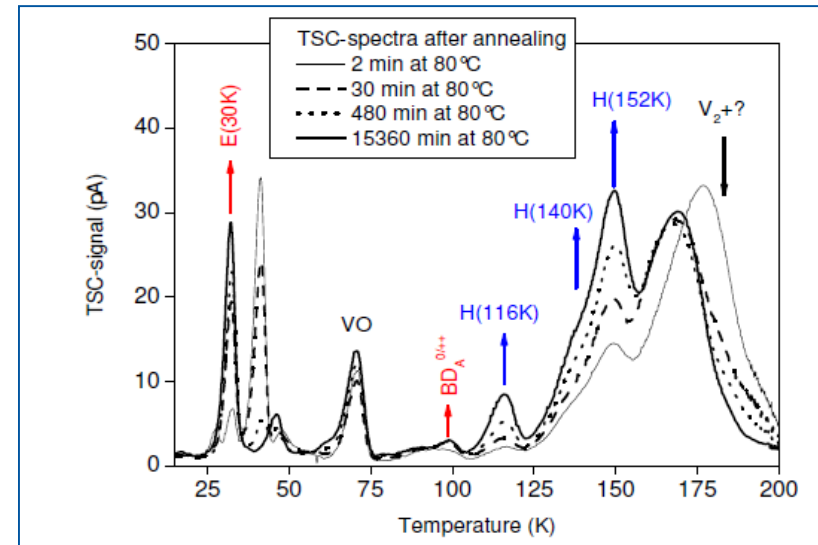
$\Delta N_t(E5)$ vs. $\Delta \alpha$
Correlation found for many materials after neutron irradiation

Defects: Impact on N_{eff} (reverse annealing)



- Macroscopic observation:
 - Irradiated silicon sensor show “reverse annealing” (negative space charge increasing with time)
 - **Example:** Neutron irradiated epitaxial silicon
 - Identification of hole traps that grow with reverse annealing and are deep acceptors (labelled: H(116K),H(140K),H(152K))
 - Absolute correlation of defect concentration to increase of $|N_{\text{eff}}|$ (reverse annealing)

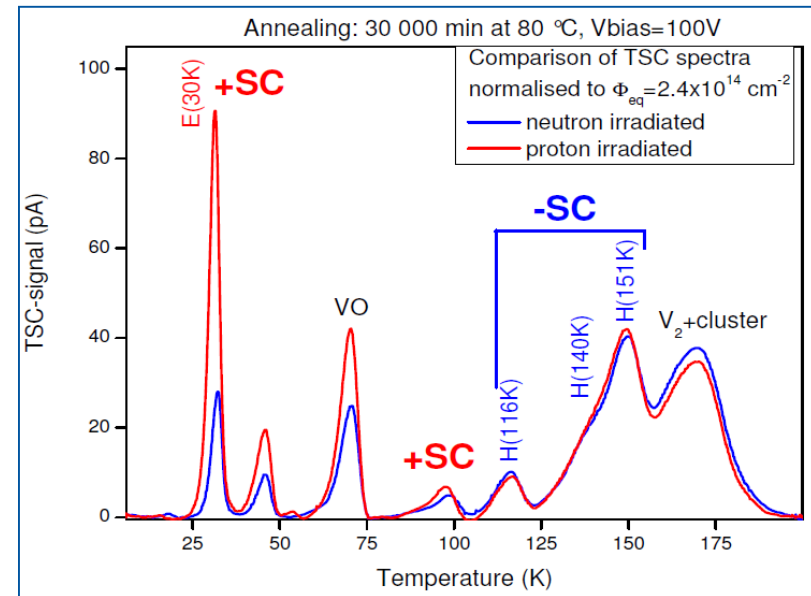
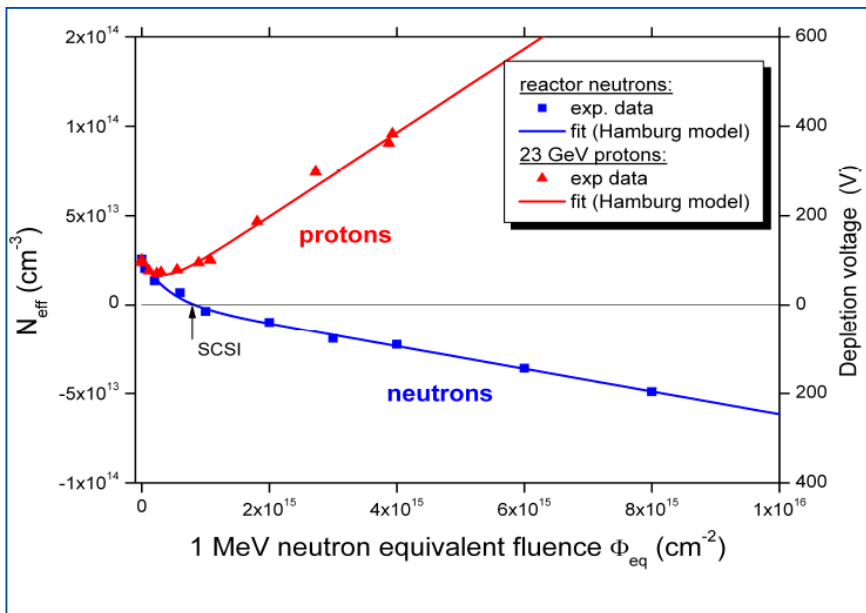
$2 \times 10^{14} \text{ n/cm}^2$, Epi-St $75 \mu\text{m}$



Defects: Impact on N_{eff} (particle type)



- Macroscopic observation: Dependence on particle type (protons vs. neutrons)
 - In several oxygen rich silicon materials neutron irradiation leads to build-up of net negative space charge (“type inversion”) while charged hadron irradiation leads to build up of net positive space charge.
 - Note: Violation of NIEL (Non Ionizing Energy Loss) Hypothesis!
- Example: Epi silicon (EPI-DO, $72\mu\text{m}$, $170\Omega\text{cm}$) irradiated with **23 GeV protons** or reactor neutrons



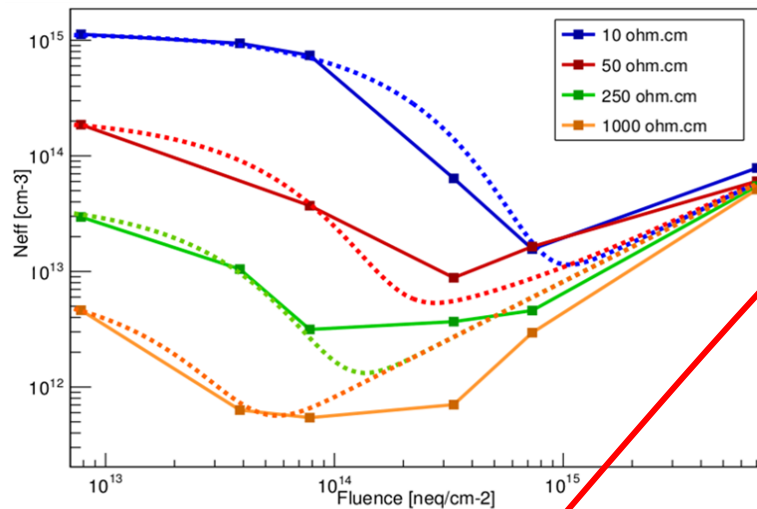
- Microscopic observation
 - The **Donor E(30K)** is introducing the additional positive space charge after proton irradiation
 - Defects related to build-up of negative space charge not influenced (follow the NIEL scaling)

RD50: Dedicated acceptor removal studies

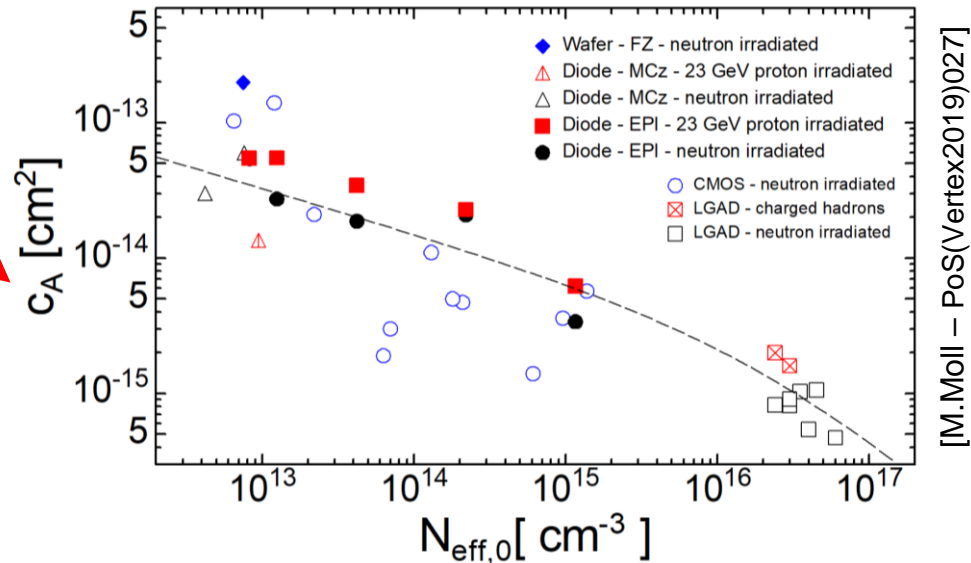


- **Acceptor removal:** Radiation induced de-activation of acceptors (p-type doping, Boron)
- **Impact:**
 - Change of silicon conductivity; Change of sensor depletion voltage and/or active volume
 - **Loss of gain in LGAD sensors**, sets radiation harness limits for timing detectors (ETL, HGTD)
- **Macroscopic studies:**

Example: 23 GeV proton irradiated epi diodes



$$N_{eff}(\Phi) = N_{B0} \exp(-c_A \Phi) + g \cdot \Phi$$



[M.Moll – PoS(Vertex2019)027]

- Acceptor removal coefficients obtained on a wide range of sensor types
 - pin diodes (epi, FZ, MCZ, ...), LGAD detectors, CMOS sensors
 - after **charged hadron irradiation (red)** and **neutron irradiation (black/blue)**

• Parameterization of acceptor removal established within RD50

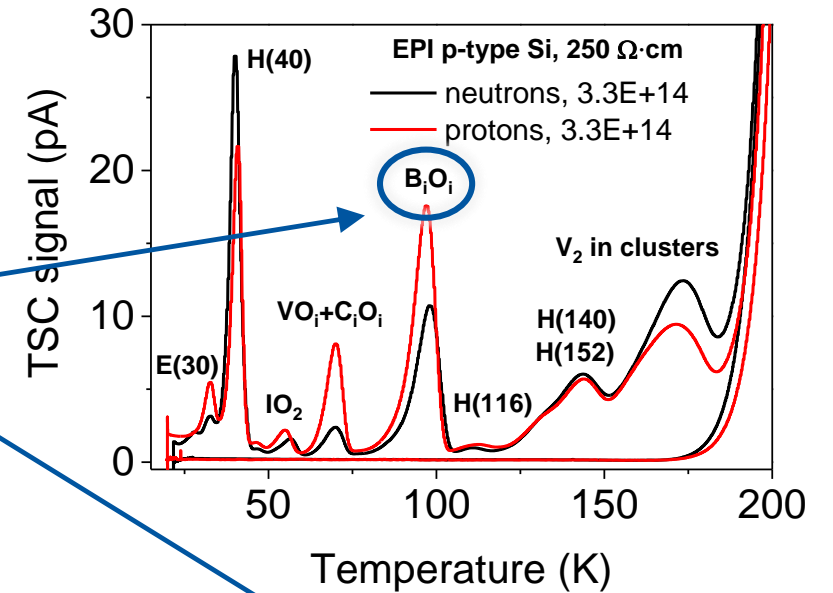
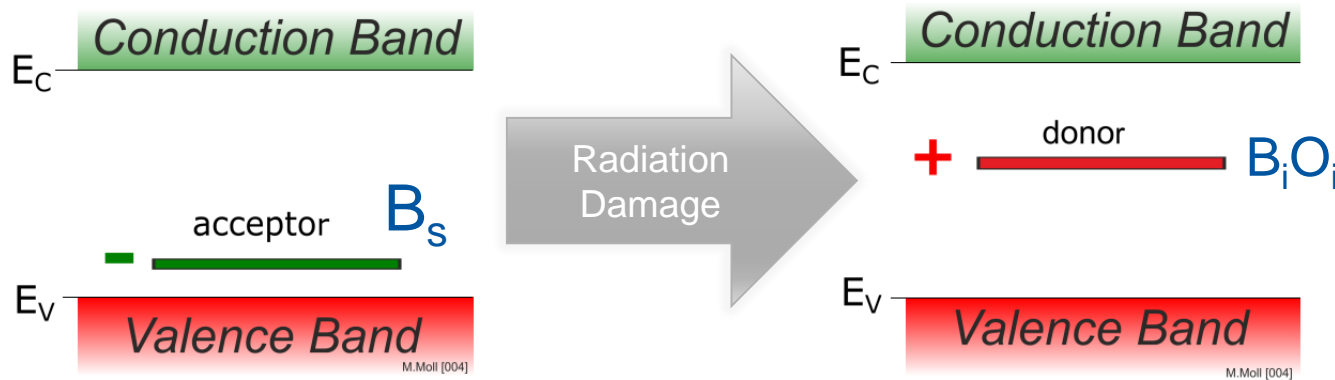
- covering the range [B]=10¹² to 10¹⁸ cm⁻³ (10 kΩcm to 5 mΩcm) i.e. damage predictions can be done

Defect studies: Acceptor Removal



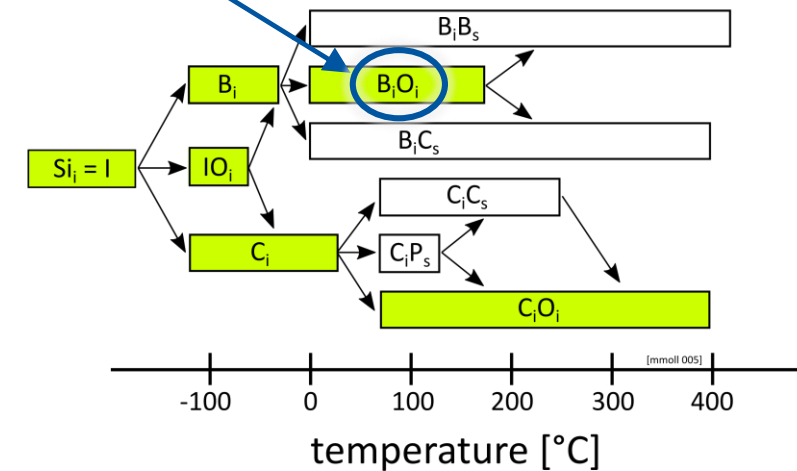
- Microscopic origin:

- Formation of defects containing Boron that no longer acts as shallow dopant



- Status

- Large amount of data (Wafers, Detectors, CMOS, LGAD)
- Acceptor removal is parametrized over 6 orders of magnitude in resistivity
 - Damage predictions are possible
- Defect engineering (with Carbon) works but microscopic understanding needs more work!
 - Measured defect concentrations do not fully explain the macroscopic observations.



Summary



Technique	Based on	Defect parameters	Limitations
C-DLTS Deep Level Transient Spectroscopy	Charge capture/emission -Capacitance transients	$E_t, \sigma_{n,p}, N_t$	low density of bulk or interface defects ($< N_d/3$) Chemical nature (indirect)
TSC Thermally Stimulated Current	Charge capture/emission Current –free charged carriers	$E_t, \sigma_{n,p}, N_t$	high density of bulk defects (up to $1000 N_d$) Chemical nature (indirect)
TDRC Thermally Dielectric Relaxation Current	Charge capture/emission Displacement Current	$E_t, \sigma_{n,p}, N_t$	high density of interface states Chemical nature (indirect)
PL –Photoluminescence	Photon Absorption followed by Photon Emission	PL bands; (E_t, τ)	Only for radiative bulk recombination centers Chemical nature (indirect)
FTIR - Infrared Spectroscopy	Absorption of IR energy on molecules vibrational modes	N_t (acc. 20-30%), Defect structure	-Large density of defects ($> 10^{15} \text{ cm}^{-3}$)
EPR Electron Paramagnetic Resonance	Zeeman effect and Spins resonance	Chemical nature and vicinity N_t	Large density of defects ($> 10^{16} \text{ cm}^{-3}$) Only paramagnetic centers
High Resolution Transmission Electron Microscopy	Electron microscopy	structure and chemical composition	Large density of defects - clusters electron beam damage of the sample during the observations

...there are many more methods (see references).

- Most powerful is the combination of various methods in combination with annealing experiments and variation of materials (e.g. doping levels, impurities, isotope doping; exposure to gammas, electrons, protons, neutrons).
- **RD50** has successfully identified several radiation induced defects responsible for device degradation effects (e.g. leakage current and effective doping of silicon sensors, impact of oxygen).
- Hot topic today: Acceptor removal ongoing work

References and Acknowledgements



Material taken from:

- RD50 collaboration: <http://www.cern.ch/rd50>
 - Anja Himmerlich, DLTS and TSC: A brief introduction, June 3-5 2020, CERN, RD50 Workshop
 - Yana Gurimskaya, I-DLTS – First experience and prospects: 17.05.2021, CERN, WP1.4. Meeting
 - Michael Moll, PhD thesis, 1999 Hamburg University
 - Gordon Davies, Photoluminescence, WODEAN workshop 2006
 - Leonid Murin, FTIR, WODEAN workshop 2006
 - Eckhart Fretwurst, DLTS, WODEAN workshop 2006
 - Ioana Pintilie, VERTEX 2016, Experimental techniques for defect characterization of highly irradiated materials and structures
- Books
 - Dieter K.Schroder, Semiconductor Material and Device Characterization
 - Gareth R. Eaton, Sandra S. Eaton, David P. Barr, Ralph T. Weber, Quantitative EPR
 - Peter Pichler, Intrinsic Point Defects, Impurities, and Their Diffusion in Silicon